

Review

# Applications of Diamond to Improve Tribological Performance in the Oil and Gas Industry

David W. Wheeler

AWE plc, Aldermaston, Reading, Berkshire RG7 4PR, UK; David.Wheeler@awe.co.uk

Received: 17 July 2018; Accepted: 28 August 2018; Published: 18 September 2018



**Abstract:** The use of diamond in tribological applications in the oil and gas industry is reviewed. The high hardness, strength, and corrosion resistance of diamond make it an attractive option for components that are susceptible to degradation by abrasive, erosive, or adhesive wear; such components may also be prone to corrosion owing to the nature of the environments to which they are often exposed. Applications such as drill bits, bearings, and mechanical seals benefit from the use of diamond, while choke valves are the subject of research programs to assess the suitability of chemical vapor deposition (CVD) diamond for these components. Also discussed are some of the conditions experienced by the components and how the properties of diamond enhance their operating lives.

**Keywords:** diamond; drills; mechanical seals; thrust bearings; tribology; valves

## 1. Introduction

Many components that form part of the equipment used in the oil and gas industry can experience extremely harsh operating environments that can significantly curtail their operating lives. The degradation processes may be tribological (e.g., abrasion, erosion, etc.), corrosion, or a combination of the two. Abrasion can result from drilling operations, while the erosion of components such as valves and pipelines can be caused by the presence of sand particles entrained in hydrocarbon fluid flows. Moreover, in oil and gas wells, other constituents may be present, many of which can be corrosive. These include salt water (commonly known as formation or produced water), carbon dioxide (CO<sub>2</sub>), and hydrogen sulfide (H<sub>2</sub>S) [1]. The high costs of premature replacement of failed equipment, and the attendant lost production render it important to find the most suitable materials to maximize the operating lives of these components.

The multifunctional nature of diamond, most notably its high hardness and strength, together with its low friction, high thermal conductivity, and chemical inertness, make it an attractive option for use in abrasive, erosive, and corrosive environments [2]. In many examples where diamond found application in the oil and gas industry, it was in the form of polycrystalline diamond (PCD), which is produced by sintering diamond grains on a cemented tungsten carbide (WC) substrate at high pressure. Presses typically apply 4–10 GPa of pressure at temperatures of between 1400 and 1800 °C [3]. Under these conditions, molten cobalt (Co), which is present as the binder phase in the substrate, infiltrates the pores between the diamond grains to facilitate the sintering process. Precipitation of carbon dissolved in the molten Co also occurs to form additional diamond grains [4]. The result is a two-phase microstructure consisting of diamond grains with a Co binder phase. Although its hardness is lower than that of natural diamond (~50 GPa), PCD has a higher fracture toughness (~8.8 vs. 3.4 MPa√m). Various grades of PCD are available depending on the grain size of the diamond, which can range from 2 to 125 μm [5]. Figure 1 shows a micrograph of the microstructure of a PCD specimen. The PCD layer, which is generally 2–4 mm in thickness [6], is bonded to a tungsten-carbide base to form what is often referred to as a polycrystalline diamond compact (PDC),

which can be easily brazed to a steel stud [7]. In the present paper, both terms are used: PCD is used when discussing the material, and PDC is used in discussions of the component/application. The two-phase microstructure of PCD can result in residual stresses caused by differences in coefficient of thermal expansion. Moreover, the presence of Co can render the PCD susceptible to transformation to graphite at elevated temperatures. In order to circumvent these problems, the PCD is sometimes subjected to a leaching treatment to remove the Co from the surface region, thereby imparting greater thermal stability [8,9]. Another approach by which the thermal stability of PCD may be enhanced is to use silicon (Si) as a binder in what is sometimes referred to as thermally stable polycrystalline diamond. During the sintering process, Si reacts with the diamond to form silicon carbide (SiC) which forms in the regions between the diamond grains. Such materials can be stable up to 1200 °C, although it has been suggested that this enhanced stability may be at the expense of lower toughness, particularly if residual Si (caused by incomplete reactive bonding during the sintering process) is present in the microstructure [10].

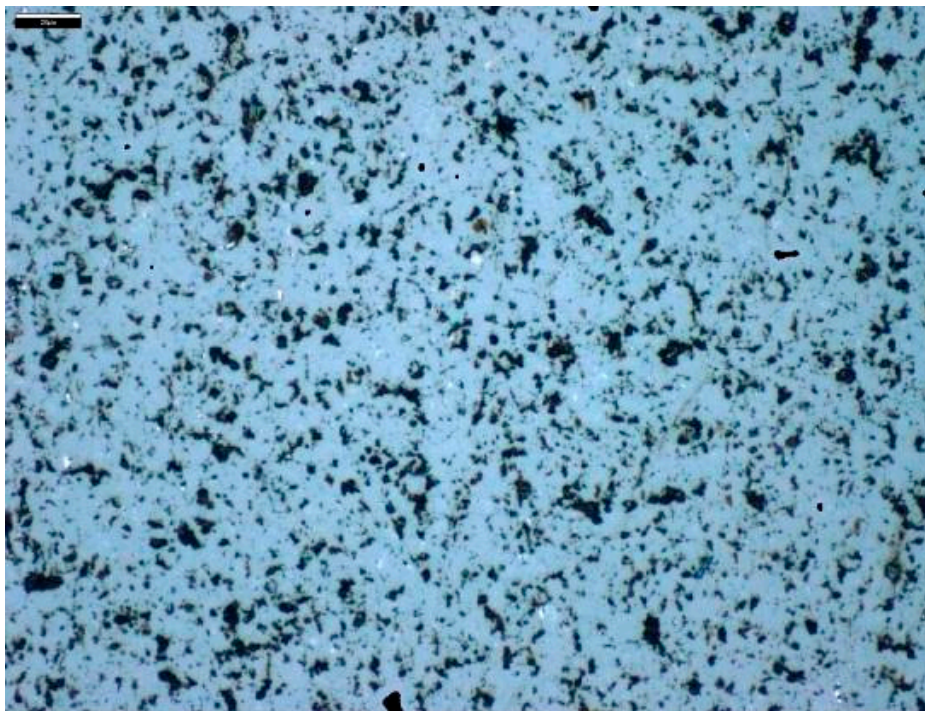


**Figure 1.** Optical micrograph showing the microstructure of polycrystalline diamond (PCD).

Another form of diamond which is used in oil and gas applications is produced by chemical vapor deposition (CVD). CVD diamond, which can be either as a thin film or in monolithic form, is deposited from the vapor phase using a hydrocarbon, such as methane ( $\text{CH}_4$ ), and hydrogen ( $\text{H}_2$ ). There are many different variants of the CVD process used to deposit diamond, the most common being microwave plasma, hot filament, and direct current (DC) arcjet [11]. The most significant difference between them is the energy source used to dissociate the reactant gases. Upon dissociation, the resultant radicals form on the substrate surface as graphite and amorphous carbon, as well as diamond. The non-diamond constituents are etched by the hydrogen gas, leaving a purely diamond deposit, although some residual graphite may still be present. The diamond deposit can range from coatings a few micrometers in thickness to bulk monolithic CVD diamond which can be up to 1 mm in thickness and 200 mm in diameter [11]. Monolithic CVD diamond can be cut (e.g., using lasers) into the desired geometry and bonded to other components, for example by brazing. Figure 2 shows an electron micrograph of the as-grown surface of a CVD diamond coating deposited on tungsten. The relevant material properties of CVD diamond and PCD are listed in Table 1 [12–24]; for comparison, the corresponding properties of a cemented tungsten carbide (WC-6Co) are also listed.

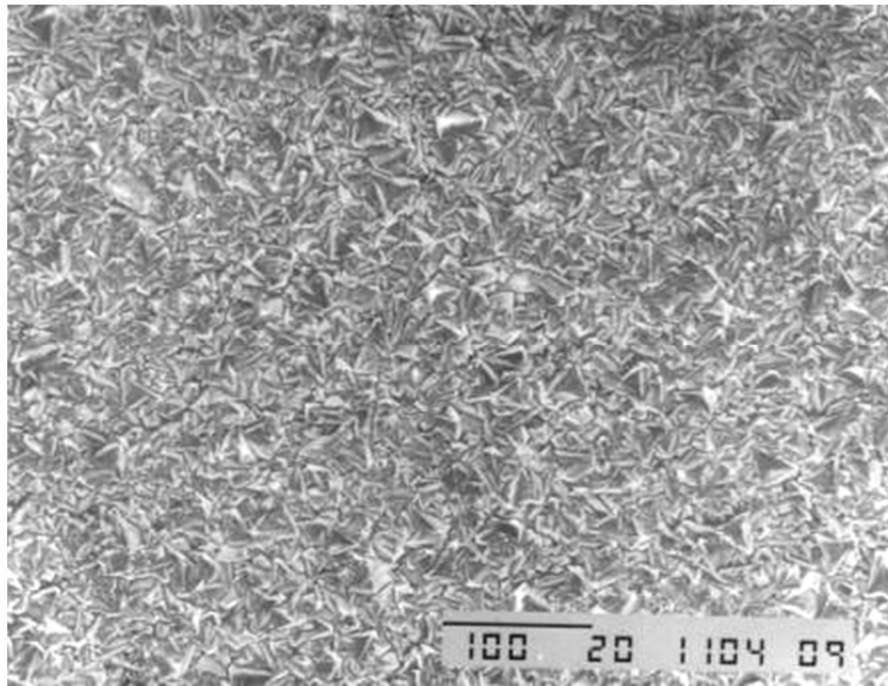


**Figure 2.** Scanning electron micrograph showing the as-grown surface of a 28- $\mu\text{m}$  chemical vapor deposition (CVD) diamond coating on a tungsten substrate.

**Table 1.** Relevant material properties of polycrystalline diamond (PCD), chemical vapor deposition (CVD) diamond, and cemented tungsten carbide (WC-6Co) [12–24].

	PCD	CVD Diamond	WC-6Co
Hardness (GPa)	53–57 [12]	60–110 [15]	14–17 [23]
Elastic modulus (GPa)	750–950 [13]	500–1200 [15]	620 [23]
Fracture toughness ( $\text{MPa}\sqrt{\text{m}}$ )	6.9–8.9 [5]	5.0–9.0 [15–18]	9.9–12.7 [23]
Poisson's ratio	0.07–0.09 [5]	0.07–0.08 [13]	0.21 [23]
Fracture strength (MPa)	444–1815 [3]	300–1200 [19]	2000–2200 [23]
Density ( $\text{kg}\cdot\text{m}^{-3}$ )	3430–4240 [13]	3520 [20]	14900 [23]
Thermal conductivity ( $\text{W}\cdot\text{m}^{-1}\cdot\text{K}^{-1}$ )	700 [14]	1646–2220 [21]	95–122 [24]
Coefficient of thermal expansion ( $\times 10^{-6}\text{K}^{-1}$ )	0.9–1.2 [14]	0.8–1.2 [22]	5.4 [23]

In this review, the use of diamond in drill bits, thrust bearings, mechanical seals, and control valves is discussed. For an application such as drilling, diamond has been used for several decades, while for mechanical seals the introduction of diamond-coated components is a more recent development. For control valves, although diamond demonstrates considerable promise, challenges such as the need to achieve an adherent diamond coating on non-planar substrates represent a continuing obstacle to its more widespread adoption.

## 2. Drill Bits

The high hardness, strength, and wear resistance of diamond make it a widely used material for oil drilling operations. Oil wells are commonly drilled to depths of over 5000 m with the diameter of the drill bit being between 20 and 400 mm [7]. In such applications, the drill bit, together with the drill collar, forms part of the bottom-hole assembly, which, along with the transition pipe and the drill pipe, make up the drill string. During the drilling process, drilling fluid (often referred to as “mud”) is pumped down the hole to the drill bit, its function being to cool and lubricate the drill bit and flush the debris created by the drilling process away from the cutter-rock interface. Drilling fluids are typically non-Newtonian suspensions composed of a base fluid, solid particles, or clays, and several additives

such as barite, gum polymers, and surfactants to increase drilling fluid performance [25]. The flow rates of these drilling fluids are typically in the range of  $10\text{--}50\text{ l}\cdot\text{s}^{-1}$  [26].

With the continuing demand for oil and natural gas, and the depletion of many of the more easily obtainable oilfields, the search for fresh reserves inevitably focuses on less accessible regions, which are often situated in more challenging environments, for example reservoirs at greater depths or more difficult geologies. Indeed, drill strings of more than 9000 m in length are used today [26].

### 2.1. Geology of Hydrocarbon Reservoirs

During the drilling process, the drill bit may pass through greatly varying geologies, which may be reflected in their different properties. Even within a single rock type, the properties can vary markedly, as shown by various workers who used techniques such as nanoindentation and atomic force microscopy (AFM) to map the variation in properties of a wide range of rocks [27–39]. In granite, which is often used in laboratory-based trials of PDC cutters (see below), Heinrichs et al. [35] showed wide variations in hardness of the three major constituents: quartz ( $H = 13 \pm 1.0$  GPa), feldspar ( $H = 10 \pm 1.0$  GPa), and biotite ( $H = 3.4 \pm 1.3$  GPa). In another study, Beste and Jacobson [27] investigated the hardness of a variety of rock types using nanoindentation. By making indents to a maximum depth of  $1\ \mu\text{m}$  (the maximum load varied between 7 and 377 mN depending on the properties of the individual rock), they mapped the hardness of a range of rocks including calcite, magnetite, hematite, sandstone, quartz, and granite. The results were compared with those recorded using micro-hardness at higher load (4.9 N). They found wide variations in hardness which were not replicated in the micro-hardness values. For example, the mean nanoindentation hardness for sandstone was 53% higher than that recorded in the micro-hardness tests. Moreover, the micro-hardness measurements could not provide an accurate indication of the full range of the hardness variations. Given the small-scale wear processes that take place at the rock-drill interface, the nanoindentation hardness values are more representative of the contact conditions than more macroscopic hardness measurements.

Such heterogeneities in the mechanical properties of rock are also seen in shale, which is a commonly encountered medium through which oil drilling operations are undertaken [40]. Shale is a multi-phase and compositionally diverse sedimentary rock which is composed primarily of sedimented clay particles, and some quantities of larger, silt-sized inclusions [28]. Measurements made by nanoindentation showed widely varying mechanical behavior, ranging from hard quartz inclusions to softer clay constituents. Liu et al. [32] performed nanoindentation on shale samples taken from the Bakken Formation, North Dakota, an area of considerable interest for hydrocarbon exploration via hydraulic fracturing. The rocks examined were found to consist principally of quartz and clay minerals (mainly illite). They found that the shale rocks exhibited considerable variation in terms of their mechanical properties, with the highest hardness and elastic modulus values recorded on the samples having the highest quartz content. Hardness values of between 1.32 and 3.08 GPa were recorded on shale specimens, although those figures masked some considerably higher hardness values in some regions of the specimens [34]. As well as having more clay minerals, the samples having the lowest hardness and elastic modulus also contained more pores and fractures than the other specimens. Heterogeneous geologies can result in more impact wear as the cutter encounters harder constituents.

The hardness of quartz is of the order of 12 GPa; the measurements made by Beste and Jacobson [27] recorded 85% of the hardness values being in the range 10–14 GPa. These values are comparable to some grades of cemented tungsten carbide, which are generally between approximately 8 and 18 GPa depending on the WC grain size and binder content [23]. As a consequence, rocks having a high quartz content are regarded as being more abrasive, causing rapid tool wear via abrasive removal of the Co binder, with subsequent loss of the WC grains [41]. Granite is typically composed of ~30% quartz and ~60% feldspar, while quartz contents of up to 97% were reported for some

sandstones [42]. Table 2 lists the mean hardness values of some commonly encountered rock types in drilling applications.

**Table 2.** Mean hardness values of commonly encountered rock types in drilling applications.

Rock Type	Mean Hardness (GPa)
Calcite	1.91 [24]
Shale	2.25 [34]
Granite	7.85 [24]
Sandstone	9.91 [24]
Quartz	11.97 [24]

In other rock formations, the host rock can also contain layers of other rock, known as stringers, of significantly different properties. For example, the overburden (the formation between the seabed and the top of the reservoir) in the Eldfisk field, which is situated in the Norwegian sector of the North Sea, predominantly consists of claystone and shale, with limestone stringers which vary in thickness between 0.3 and 5.2 m with an average of 0.9 m [43]. Calcite, which is a major constituent of limestone, can have a compressive strength in excess of 260 MPa; in contrast, the corresponding figure for shale is in the region of 34 MPa [44]. Such variations in properties will render the drill bit susceptible to impact damage and present further challenges to its continuing effective operation.

It can therefore be seen that many rock types, particularly the harder formations, can be extremely abrasive. In abrasion, a significant factor influencing the wear rate is the ratio of the surface hardness ( $H_s$ ) to that of the abrasive hardness ( $H_a$ ). For full abrasive cutting to occur,  $H_a$  must be greater than  $1.2H_s$ ; as the surface hardness, or even that of large second-phase particles in the surface approaches that of the abrasive, wear rates fall substantially [45]. Empirically, abrasive wear rates were found to decrease from an essentially constant value at  $H_s/H_a < 0.65$ – $0.75$  to a very low value at  $H_s/H_a > 1.2$  [46]. However, in materials such as cemented WC or PCD, the microstructures of which both consist of hard WC or diamond grains in a binder phase such as Co, abrasion of the softer binder phase can result in removal of the harder phase.

During the drilling process, rock is fragmented by a combination of crushing, scraping, gouging, and impact [41]. The particular mechanism(s) of rock removal during a drilling operation can vary depending on the design of the drill bit employed and the properties of the rock being drilled. One way by which drilling performance may be quantified is the rate of penetration (ROP), which is defined as the drilled distance per unit time. As a guide,  $50$ – $60 \text{ m}\cdot\text{h}^{-1}$  is a good ROP [47], although this can drop significantly when the drill encounters a harder constituent in a softer rock formation, for example limestone in shale [43]. The weight on bit (WOB) ranges from 0 to 250 kN, while the torque on bit (TOB) is in the range of  $0.5$ – $10 \text{ kNm}$  [26].

Drill bits can degrade via a number of ways, including tooth loss, tooth fracture, tooth wear, and bit balling [48]. The last of these occurs when drilling debris becomes adhered to the drill bit, thereby impairing the ability of the drill to penetrate the rock. Drill bit wear is manifested in the form of diminishing ROP and increases in torque, which necessitates bit replacement when these parameters reach unacceptable levels.

## 2.2. Drill Bit Design

There are several different bit designs that are used in oil drilling operations, two of the most common being the roller-cone and the rotary-drag bits. The roller-cone design consists of (most commonly) three rotating cones on which teeth (usually steel or WC) are mounted and intermesh with each other. The rotating cones remove rock from the drilling zone by crushing, chipping, and gouging, the relative proportions of which are dependent on the properties of the rock being drilled, with harder formations requiring more crushing [41]. However, in hard-rock drilling environments, roller-cone drill bits suffer extremely short lives owing to rapid wear of the bearings that support the roller cones [49].

The other common drill design is the rotary-drag (or fixed-cutter) bit, which contains an array of teeth and drills rock under a constant thrust force with continuous rotation [41]. It removes material using one or more of three mechanisms: dislodging in granular rock, shearing of brittle rock, and ploughing [41]. The majority of diamond drill bits are of the drag-bit design.

Prior to the introduction of diamond drill bits, the most common bit materials were nickel-chromium-molybdenum (Ni-Cr-Mo) steel (e.g., AISI 4815 and AISI 8720), which were carburized to impart greater wear resistance, and cemented tungsten carbide (WC) with cobalt-binder contents of between 6% and 16% [41]. However, the rapid wear of these materials in the most abrasive rocks limited the distance they could drill before replacement became necessary. Given the costs involved in replacing a worn drill bit, especially in a deep well, as well as lost productivity, there was a strong economic incentive to introduce innovations through which greater rates of penetration and increased bit life could be achieved.

Diamond has been used in oil drilling applications for more than a century. According to one account, diamond drill bits were first used to drill for oil in 1863 [50]. However, full-hole diamond bits for oilfield drilling were first commercially introduced in the early 1950s [51]. For these applications, diamond is used in two forms. One is a surface-set drill bit in which a single layer of diamonds is mounted in a matrix on the crown of the drill. The other is the PDC bit, which consists of multiple PDC cutters attached to a solid bit head and arranged about the rotational axis of the bit [49]. Indeed, one design of drill bit contains 48 face cutters [52]. An example of a PDC cutter is shown in Figure 3. The PDC cutters are generally of a cylindrical geometry (the diameters generally vary between 8 and 24 mm) and are generally chamfered to increase the cutter's impact resistance [53]. A schematic diagram of a PDC drill bit can be seen in Figure 4 [54]. Since its commercial introduction in the 1970s, the PDC bit has progressively eclipsed the surface-set diamond bit in many drilling applications.



**Figure 3.** A polycrystalline diamond compact (PDC) cutter consisting of a polycrystalline diamond layer on a tungsten-carbide substrate. Image used with permission of the Element Six Group, Copyright © Element Six Group, 2017.

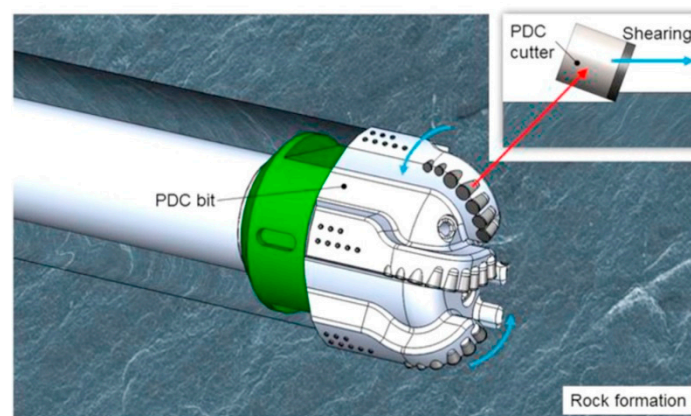


**Figure 4.** Diagram showing rock drilling performed with a commercial PDC bit [54].

Under field conditions, the velocity of the PDC cutters typically ranges from 1.6 to 4 m·s<sup>-1</sup> with bit rotation speeds of 60–250 rpm depending on the bit dimension, hardness of the rock formation, and cooling mode [55]. With a typical penetration ranging from 15 to 60 m·h<sup>-1</sup>, and an average rotation speed of 120 rpm, the penetration per revolution ranges from 2 to 8 mm [56].

One of the advantages of PDC drill bits is that they remove material via a shearing process which is more energy efficient than the compressive stresses generated by roller-cone bits. In shear, the energy required to reach the plastic limit for rupture is significantly less than by compressive stress. PDC bits, therefore, require a lower WOB than roller-cone bits [57]. As a result, rock removal by shearing requires only 15–20% of the energy required by crushing and grinding, thereby giving PDC bits the potential to drill much more quickly and efficiently than conventional bits [58]. A sharp PDC bit will typically drill two to three times faster than the best roller-cone bit in soft formations, although such performance will gradually decline with increasing wear [56]. The greater efficiency offered by PDC bits led to their use in drilling long sections of homogeneous rocks of low shear strength. In the northern North Sea, long homogeneous claystone sections proved ideal formations for PDC, leading to rates of penetration up to three times greater than those obtainable by roller-cone bits and with greatly extended bit life [59].

### 2.3. Tribological Performance of PDC Drill Bits

There are various laboratory-based test methods that are used to assess the performance of PDC drill bits. One of the most widely used is the vertical turret lathe (VTL), in which the cutter is mounted above a cylindrical block of rock (e.g., granite) which rotates about a vertical axis. The cutter machines the top surface of the rotating rock at a defined depth of cut. As the cutter traverses from the outer surface to the center of the rock, the rotation speed of the rock is increased in order to keep the speed at the cutter constant. During the cutting process, the components of the cutting reaction forces are measured via a load cell mounted on the vertical axis of the lathe. However, the cutting conditions in the VTL test are less than representative of those encountered in actual drilling operations.

An alternative laboratory test that is used to assess cutter performance is bit cutter on rock tribometry (B-CORT), which is based on the pin-on-disc geometry. In the test, a cutter is loaded onto the surface of a rotating disc made from rock, and parameters such as the frictional cutting force at the cutter–rock interface, linear disc speed, and depth of cut (DOC) are measured in situ to understand the impact of these tribological parameters during a simulated drilling process [60]. B-CORT was used to evaluate the behavior of PDC in the cutting of shale, marble, and sandstone under dry conditions and in the presence of water [61]. The cutting tests were carried out at a speed of 0.46 m·s<sup>-1</sup>, a rake angle of 20°, and at four different loads. They found significant differences between the different rocks under dry and water-lubricated conditions. For the dry cutting of marble, the coefficient of friction, after initially being in the range of 0.75–0.80, stabilized at ~0.65 irrespective of load. When water was used as a lubricant, similar trends were observed, although this time the steady-state coefficient of friction was reduced to between 0.15 and 0.20. For sandstone and shale, the effect was less pronounced, with different behavior observed at different loads. One notable observation was that, despite reducing the coefficient of friction, the presence of water had the effect, in some cases, of increasing the ROP. This was attributed to weakening of the rock by the water which could occur via penetration of the pores, increasing pore pressure and reducing intergranular cohesion [61]. This was seen for the cutting of sandstone and shale, although, in the case of the latter, the coefficient of friction was greater in the lubricated tests.

### 2.4. Wear Mechanisms of PDC Drill Bits

During the drilling process, the drill bit will experience a range of conditions including abrasion, impact, vibration, and fatigue, all of which have the potential to cause its degradation and premature failure. Moreover, owing to the presence of corrosive constituents in the drilling fluid, it may also

be vulnerable to corrosion. Erosion can also be a problem if drilling debris becomes entrained in the drilling fluid, resulting in erosion of the drill bit and other parts of the bottom-hole assembly.

The most common wear mechanisms experienced by PDC drill bits are abrasion, impact, and thermal degradation. During the drilling operation, as wear of the drill bit increases, the efficiency of the shearing process (by which material is removed) declines. In an attempt to compensate for this deterioration in performance, drillers may increase the WOB to maintain the ROP [6,62]. However, this can accelerate the wear of the cutter edges and further impair drilling efficiency as the action of material removal by the worn drill bit changes from shearing to crushing of the rock. Moreover, the frictional energy generated by the increased WOB can result in high temperatures, which can cause thermal degradation of the PCD [6]. The most prominent wear mechanisms are discussed in more detail below.

#### 2.4.1. Abrasion

The most common wear mechanism operating on PDC bits during rock drilling is abrasion [63,64]. This causes the formation of a flattened region on the cutter [65], and the friction on the wear flat can dissipate up to 50% of the total energy for drilling [56]. Although the hardness of diamond is considerably higher than that of the commonly encountered rocks drilled by PDC cutters, it can still be subjected to abrasion during the drilling process. The mechanisms via which the abrasion occurs were studied using laboratory-based abrasion tests. In one such test, ASTM B611, in which the specimen is loaded against a rotating steel wheel in the presence of an abrasive slurry, PCD was shown to undergo abrasion via the removal of regions of the Co binder. This results in shallow grooves, which are subsequently filled by abrasive particles from the slurry and confer a degree of protection to the underlying regions of Co. In addition, the presence of cracking was observed in the diamond grains, a finding ascribed to the effects of impact loading and fatigue [66]. In a recent comparison of the abrasive wear performance of PCD with various grades of cemented WC and WC-Co/diamond composite materials, PCD was shown to offer significantly greater wear resistance than all other materials tested [66].

One of the factors affecting the wear rate of PCD is grain size. In turning tests against granite in a lathe, Miess and Rai [67] found that wear resistance decreases with increasing grain size for PDC tools with mean grain sizes ranging from 2 to 120  $\mu\text{m}$ . However, this is not the only variable influencing its performance. Yahiaoui et al. [52] compared the performance of six different PDC cutters of different grain sizes, some of which also underwent a leaching process to remove the Co binder from the PDC surface regions. They tested the PDC specimens against a manufactured mortar rock counterface at a speed of  $1.8 \text{ m}\cdot\text{s}^{-1}$ ; no lubricant was used in the tests. They used a quality factor ( $Q$ )—a dimensionless value dependent on parameters such as coefficient of friction, intrinsic specific energy, cutting capacity, and wear rate—to rank the various cutters in terms of performance. The PDC cutter having the highest quality factor had a mean grain size of  $13.3 \pm 3.9 \mu\text{m}$ , and was leached to a depth of 70  $\mu\text{m}$ . The authors averred that fine-grained PDC exhibited the lowest wear rates. However, this assertion did not appear to be borne out by the data, which showed that PDC cutters having smaller grain sizes (ranging from 8.1 to 11.6  $\mu\text{m}$ ) exhibited higher wear rates, although the size distribution of the best-performing cutter was the narrowest of the six. Leaching also appeared to enhance the wear performance with the top three PDC cutters all having been leached to various depths ranging from 70 to 325  $\mu\text{m}$ .

Yahiaoui et al. [68] also carried out a subsequent investigation into the performance of a range of PDC cutters of different grain sizes and process conditions in contact with a manufactured mortar counterface, the quartz content of which was 60 wt %. The tests were carried out under similar conditions to the previous study [52]. The principal wear mechanism was found to be abrasion caused by micro-cutting from the quartz particles from the rock, which generated both intergranular and transgranular cracking in the diamond grains, as well as removal of the more ductile Co phase. This damage resulted in the loss of diamond grains from the PDC microstructure. Quartz particles were also seen to become embedded in the PDC surface, a finding indicated by both optical microscopy and X-ray diffraction (XRD). The PDC cutter offering the most abrasion resistance had a larger grain size ( $17 \pm 4 \mu\text{m}$ ) and was sintered at a higher pressure for a shorter period of time.

#### 2.4.2. Impact

Although PDC drill bits exhibit high resistance to abrasive wear, they are susceptible to impact damage on account of their low fracture toughness. During drilling, impacts can occur as a result of contact between the cutter and the side of the drilled hole. A whirling bit drills a multisided polygon-shaped hole rather than a round one, which can result in severe impact damage to the cutters [40]. Another way by which the cutter can suffer impact damage is through contact with harder constituents in softer rock. The repeated impacts of the cutter on the rock can cause the initiation of microscopic fatigue cracks, the propagation of which can result in the chipping and spalling of fragments from the cutter.

Kanyanta et al. [69] studied the impact fatigue of PDC, and showed that grain size could influence the fatigue behavior, with larger grain-size grades offering greater fatigue resistance. They developed an in-house cyclic impact test facility and compared the impact behavior of two grades of PDC of different grain sizes (mean grain sizes of 6 and 30  $\mu\text{m}$ ). During the tests, the repeated impacts caused the formation of circular cracks that formed on the PDC surface just outside the region of contact. As the impacts continued, these cracks propagated through the PDC layer at an angle of between  $40^\circ$  and  $47^\circ$  to the surface. The final stage of the impact fatigue process was catastrophic failure. The larger-grain-size PDC was found to offer up to 70% better impact fracture resistance than its smaller-grain-size counterpart. The fatigue limit of the coarser-grain-size PDC was also 10–15% higher than the finer-grain-size grade.

Garcia-Marro et al. [70] investigated the effect of cyclic contact loading via a spherical WC indenter on the residual strength of PCD specimens with mean diamond grain sizes ranging from 4 to 20  $\mu\text{m}$ . The effect of the repeated loading was evaluated by performing biaxial flexural testing of indented specimens and comparing the results with those measured on specimens that were not indented. They found that small-grain-size specimens exhibited higher strengths; however, with increasing number of loading cycles, the residual strength declined markedly. In contrast, the larger-grain-size specimens displayed a greater tolerance to damage, which was indicated by much lower reductions in strength with increasing number of loading cycles.

Although larger-grain-size PCD shows superior impact and fatigue resistance, some studies indicated that a smaller grain size offers better abrasion resistance. Therefore, the selection of the optimal microstructure for a drill bit is likely to be a trade-off between impact resistance and abrasion resistance.

In recent years, the development of conical diamond elements (CDE), in which the diamond thickness is significantly greater in some regions, resulted in enhanced impact strength and abrasion resistance [6]. This was demonstrated by Azar et al. [44] who described a comparison of the impact performance of a CDE and a conventional PDC cutter element. The conventional cutter failed on the first impact, while the conical element remained undamaged after more than 100 impacts. Other advantages of the CDE design include greater wear resistance and cutting efficiency, as well as more efficient dissipation of frictional heat than conventional PDC cutters. Figure 5 shows an example of shaped diamond cutters used in PDC drill bits.



**Figure 5.** Shaped diamond cutters used in PDC drill bits. Image used with permission of the Element Six Group, Copyright © Element Six Group, 2017.

### 2.4.3. Thermal Degradation

The friction resulting from the cutting process can lead to the generation of high temperatures, which can cause thermal degradation of the PDC. The presence of Co, which can aid the sintering process during the manufacture of PDC, can also catalyze the transformation of diamond to graphite at high temperatures [71]. In air, the onset of damage appears to occur at approximately 600 °C and is accompanied by extrusion of the binder phase from the PDC surface, the extent of which is dependent on the binder content in the PDC [67]. However, a deterioration in cutter performance is observed at much lower temperatures. Indeed, an acceleration in the wear rate is observed in PDC cutters when the temperature exceeds 350 °C [49]. Mehan and Hibbs [8] showed that PCD specimens heated to approximately 870 °C in an inert atmosphere exhibited thermal degradation, which was attributed to graphitization. After an incubation period, the length of which was dependent on the temperature and thermal degradation, initially in the form of intergranular cracking, but later, transgranular cracking, was observed in polished metallographic sections of the specimens prepared after the tests.

In addition to the transformation of diamond to graphite, high temperatures can also result in rapid wear due to the formation of cracking caused by differences in thermal expansion coefficient between diamond and the Co binder. This differential thermal expansion may also affect the strength of the bond between the PCD layer and the WC substrate [57].

Westraadt et al. [71] studied the thermal degradation of PCD when used in the machining of granite. In the tests, which were conducted under dry conditions, thermocouples mounted on the diamond surfaces recorded temperatures in excess of 500 °C. As a consequence, cracks (largely intergranular) were observed extending from the surface into the interior of the material. Such cracking was responsible for a deterioration in the performance of the tool, and eventually, its failure. Transmission electron microscopy (TEM)—including electron energy loss spectroscopy (EELS)—of samples taken from these regions of the PCD indicated the presence of graphite, as well as cobalt and diamond. The authors attributed the formation of graphite to the high temperatures generated by the cutting process.

In their study of the wear behavior of PDC cutters sliding against a manufactured mortar rock counterface, Yahiaoui et al. [68] found that, in addition to abrasion of the PDC from the quartz particles, there was evidence of transformation from diamond to graphite or amorphous carbon. Raman spectra acquired from the worn PDC surfaces showed peaks at 1359 and 1580  $\text{cm}^{-1}$ , both indicative of  $\text{sp}^2$  bonding (i.e., graphite). The diamond peak at 1332  $\text{cm}^{-1}$  also underwent a small shift compared to the unworn PDC, which was attributed to relaxation of the residual stresses during the wear process. The transformation to graphite will also result in a deterioration in cutter performance.

Several researchers have investigated the effect of removing the Co binder from the surface on the thermal stability of the PCD. Methods included leaching using an HF/HNO<sub>3</sub> solution [8] and electrolysis [9]. Mehan and Hibbs [8] found that the cracking seen in heated PCD specimens was not observed in leached specimens. Liu et al. [9] investigated the wear resistance of PCD specimens from which the Co was removed; the depth of the removed region ranged between 50 and 300  $\mu\text{m}$ . In turning tests against granite, the removal of Co was found to result in a significant increase in wear resistance. XRD of wear surfaces of treated and untreated PCD specimens revealed the presence of graphite on the untreated specimen; however, on the treated specimen, from which the Co was removed from the surface region, no graphite was detected. This finding led the authors to suggest that graphitization was the primary wear mechanism in specimens in which Co was present at the surface.

### 2.5. Performance of PDC Drill Bits

The introduction of PDC drill bits has resulted in a significant improvement in drilling performance. According to one study in the late 1990s, which compared performance improvements in the PDC drill bits with those for roller-cone bits, although both types of bits showed improved rates of penetration, the ROP increase for roller-cone bits was 11%, while, for PDC bits, the corresponding

figure was 57%. In terms of bit life, the margin of superiority for PDC bits was even greater: 115% vs. 19% for roller-cone bits [40].

Miyazaki et al. [72] compared the drilling performance of a PDC percussion drill bit with one containing cemented tungsten carbide (WC-Co) cutters. The tests were conducted on a drill test apparatus, and bit performance was compared in the drilling of two types of granite in the presence of water as a drilling fluid. The PDC drill bits were found to outperform the WC bits in terms of bit wear, torque on bit, rate of penetration, and specific energy. For each of these parameters, the PDC bit showed a gentle increase (or decrease in the case of ROP) over the course of the test. However, for the WC-Co bit, the rate of change of these parameters was significantly greater than that of the PDC bit. For the bit wear, defined in this case as height loss of gauge tip normalized to original tip height ( $\Delta h/h_0$ ), the value for the PDC bit was only one-third of that for the WC-Co bit. The PDC bit was shown to offer greater efficiencies in the drilling process, both in terms of greater rates of penetration and reduced energy required to drill a unit volume of rock, as well as longer bit life, making bit replacement less frequent, thereby reducing costs.

In one gas drilling application that benefitted from the adoption of PDC bits, the previously employed steel roller-cone drill bits only achieved rates of penetration of  $3.6 \text{ m}\cdot\text{h}^{-1}$ , with bit balling a frequent problem. However, when PDC drill bits were adopted, mean ROP improved by a factor of three, despite the presence of limestone layers in the rock formation; a further benefit was that the problem of bit balling was largely eliminated [58].

Improvements to drill bit design were also made in recent years, and this resulted in improvements to drilling performance. Some of these have been described by Scott [40]. These included diamond-enhanced inserts in roller cones. An example of a diamond insert used in a roller-cone bit can be seen in Figure 6. Although the costs of these diamond-enhanced inserts are significantly greater than tungsten carbide (initially by a factor of between 50 and 100), this cost difference declined as the technology has become more widely adopted. However, the higher costs can often be justified by the improved productivity that they offer.



**Figure 6.** A diamond insert used in a roller-cone drill bit. Image used with permission of the Element Six Group, Copyright © Element Six Group, 2017.

After their commercial introduction in 1976, the initial adoption of PDC drill bits was slow. In 1980, they accounted for less than 2% of the total footage drilled, and, a decade later, this only increased to just over 5% [40]. Since that time, the use of PDC has become increasingly widespread, and, by 2010, PDC bits accounted for 65% of footage drilled in oil and gas applications [73], a figure which was predicted to rise to 80% by 2020 [74].

### 3. Bearings

In addition to its high wear resistance, another attribute of diamond that is of relevance to tribological applications is its low-friction behavior. Natural diamond exhibits a low coefficient of friction ( $\mu$ ) when sliding against itself, and, with the exception of high vacuum, where  $\mu$  can exceed 1.0, values of between 0.05 and 0.15 have been recorded in most environments [75]. PCD was also observed to exhibit similar behavior, although it is dependent on factors such as surface roughness. Nevertheless, one application where this advantageous characteristic was exploited is in thrust bearings which are used in down-hole drilling motors. In many drilling applications, the drill bit is attached to a hydraulic motor which is powered by drilling fluid (mud) that is pumped down a pipe connected to the motor. The drilling fluid is conveyed back to the surface via the annulus surrounding the pipe in the bore hole. One advantage of such an arrangement is that it avoids the need to rotate the entire drill string.

The operating conditions experienced by components of such motors can be extremely arduous, involving high dynamic loads and vibrations. In one study, it was found that when the drill bit bounced off the bottom of the hole, loads of more than three times that of the applied bit weight were generated [76]. Moreover, the bearing surface speed can be up to  $6.5 \text{ m}\cdot\text{s}^{-1}$  and specific loading can be up to 70 MPa [77]. Ideally, the operating life of the bearing assembly must be at least commensurate with that of the drill bit; however, under severe conditions, it may only be 250 h [78]. There are alternatives to diamond thrust bearings, including rolling-element (ball) bearings and tapered roller bearings; however, the former are susceptible to erosion, while the latter must be sealed from the drilling fluid and pressure compensating the bearing assembly [79].

Diamond is an advantageous material for this application for a number of reasons: (i) its low friction behavior; (ii) high hardness (making it more resistant to abrasion from drilling debris in the drilling fluid); and (iii) high thermal conductivity, which is more than an order of magnitude higher than that of steel (e.g., AISI 4140), and therefore enables greater dissipation of heat generated by friction and reduces the heat build-up in the bearings, which can promote oxidation or graphitization of the diamond. A common design of PDC bearing consists of an array of round PDC pads mounted onto a ring. Two rings are used in operation, one of which remains stationary, while the other rotates with the rotor [80]. Figure 7 shows an example of a thrust bearing [77].



Figure 7. A PDC thrust bearing [77].

Sexton and Cooley [79] used a bearing test apparatus to evaluate the performance of PDC thrust bearings. They found that the coefficient of friction of PDC sliding against itself in water was between 0.05 and 0.08. In a subsequent study, Knuteson et al. [77] examined the running-in behavior of PDC

thrust bearings by testing them in a thrust bearing test apparatus at a sliding speed of  $2.0 \text{ m}\cdot\text{s}^{-1}$  for a total period of 72 h. Over this time the coefficient of friction was observed to decrease from initial values of between 0.05 and 0.11 down to as low as 0.015; this was accompanied by a reduction in surface roughness ( $R_a$ ) of the bearings from approximately  $1.0 \text{ }\mu\text{m}$  (the untested surface) to a mean value of  $0.12 \text{ }\mu\text{m}$ . For comparison, the authors also examined the surface of a used PDC bearing from a drilling turbine that achieved approximately 1000 h down-hole service; the  $R_a$  of the PDC pad was  $0.04 \text{ }\mu\text{m}$ . The authors suggested that these changes represented changes to the lubrication regime from the initial boundary conditions to a more mixed-mode regime. Such conditions would serve to result in significantly longer operating lives. Owing to the high initial costs of diamond thrust bearings, bearing life must be between five and ten times longer than that of conventional bearings in order to justify the greater initial expense [79]. However, in some drilling applications, a bearing life of over 3000 h has been observed [77].

#### 4. Mechanical Seals

Like PCD, described in the previous section, CVD diamond coatings also exhibit a low coefficient of friction in most environments, although it is dependent on factors such as surface roughness [81,82]. Figure 8 shows a surface profile of an as-deposited CVD diamond coating (thickness  $20 \text{ }\mu\text{m}$ ) on WC. The surface roughness of such a coating can be as high as  $5 \text{ }\mu\text{m}$ , which, in sliding contact with a softer counterface, can be extremely abrasive, leading to high friction and wear. Although this can be overcome by lapping and/or polishing of the diamond film, such processes can be time consuming and are not practicable for non-planar geometries. One way by which the need for a polished diamond surface can be avoided is to deposit nanocrystalline (sometimes dubbed “ultrananocrystalline”) diamond coatings, which can have  $R_a$  values of 20–30 nm and an average grain size in the range of 2–5 nm [83].

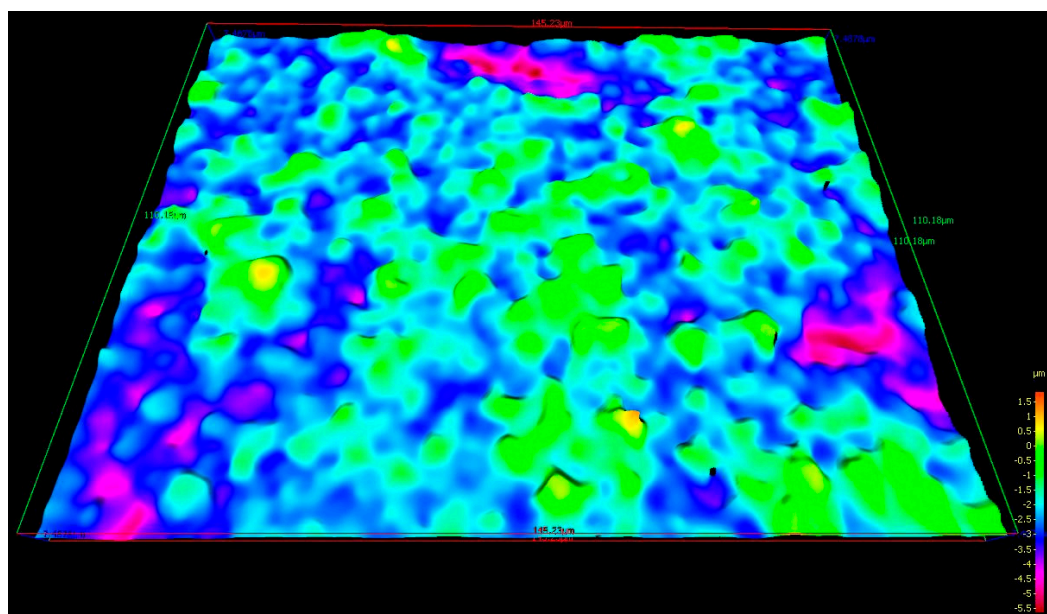


**Figure 8.** Surface profile of an as-deposited 20- $\mu\text{m}$  CVD diamond coating on tungsten carbide.

A common observation in tests of CVD diamond sliding against itself is an initially high coefficient of friction, which decreases as the test proceeds. Such behavior is particularly evident in tests of as-grown micro-crystalline diamond films, and was attributed to the mechanical interlocking of surface asperities [84–86]. Over time, these asperities become more truncated, which results in a decrease in surface roughness. Any large particles of wear debris that may be present can cause grooving of the coating surface, and self-polishing by two- and three-body abrasion also occurs [87]. The reduction in

surface roughness is accompanied by a decrease in the coefficient of friction until the establishment of steady-state sliding conditions. An example of this can be found in the work of Bull et al. [82], who tested as-grown CVD diamond on Si substrates. The initial coefficient was approximately 0.35, which declined and stabilized between 0.1 and 0.2. Upon steady-state conditions being achieved, significant changes to the coefficient of friction are not generally observed, although subsequent increases may be seen in the event of, for example, coating failure.

CVD diamond coatings found application as coatings for mechanical seals which are used in components such as pumps to seal rotating shafts. A mechanical seal consists of a sealing interface located between a pair of radial faces, one rotating and the other stationary. The lubrication regime is often the mixed or boundary conditions with the working fluid acting as the lubricant [88]. Between the two counterfaces, the sealed fluid penetrates the interface and is responsible for supporting most, if not all, the load. The fluid is often low viscosity, typically aqueous or a hydrocarbon, but it can be any fluid that can be pumped. It can also be above its atmospheric boiling point. It is important to maintain the correct film thickness; this figure is generally in the region of between 0.25 and 8  $\mu\text{m}$  [89]. Films that are too thin are insufficient to prevent direct contact between the two counterfaces, generating excessive heat and high rates of wear. Films that are too thick will result in unacceptably high leakage [90]. Although mechanical seals do not normally operate under dry sliding, such conditions are often encountered intermittently, particularly during the start-up phase of operation. While it is difficult to generalize, it is instructive to consider the typical conditions witnessed by the majority of mechanical seals. The net specific load is usually between 0.1 and 5 MPa, while the sliding speed is within the range of 1–20  $\text{m}\cdot\text{s}^{-1}$ . The temperature of the sealed fluid can be from 20 to 300  $^{\circ}\text{C}$  [91]. In defining the operating envelope for a mechanical seal, a common parameter that is used is the maximum  $PV$  value, where  $P$  is the pressure drop across the seal, and  $V$  is the mean sliding velocity at the interface in meters per second [89]. However, it is only for a specified fluid at a specified temperature [91].

According to the United States Department of Energy, over 50% of pump life-cycle costs result from energy and maintenance expenses, and energy savings of 20% or more are possible with systems optimization [92]. Diamond coatings are an attractive option for mechanical seals for two reasons: (i) high wear resistance; and (ii) low friction behavior. Their high wear resistance (resulting from high hardness) is not only when sliding against the counterface, but also, for pumps handling multi-phase service, the sealed fluid may contain suspended or dissolved solids and/or bubbles which can be abrasive or erosive. Furthermore, the high thermal conductivity of diamond reduces the heat generation, which can cause thermal distortion of the seal faces and result in unacceptable leakage rates. Mechanical seal failures are responsible for over 70% of pump problems [93], and therefore, there are clear potential benefits arising from any improvements that can be made to the operating lives of mechanical seals. The other desirable attribute of diamond coatings—their low friction behavior—can reduce frictional losses, and thus, energy consumption. Diamond, therefore, has the potential to prolong seal operating life through lower wear rates, as well as to reduce power consumption.

A wide variety of materials are used in mechanical seals including carbon-graphite, WC, alumina ( $\text{Al}_2\text{O}_3$ ), and SiC. One commonly employed combination of seal face materials is carbon-graphite running against SiC [94]. The low cost, chemical inertness, and self-lubricating properties of carbon-graphite renders it particularly suitable in many applications [95]; however, it can be susceptible to wear in more abrasive environments. In such cases, a more wear-resistant alternative is an SiC/SiC combination, although high friction and rapid wear can occur if the lubrication in the sealing gap is inadequate.

Diamond began being investigated as a potential seal material in the 1990s. A number of laboratory-based tribological tests were employed to evaluate the efficacy of diamond as a mechanical seal material. These included the pin-on-disc, thrust-washer, and ring-on-ring tests. Although pin-on-disc is a widely used tribological test, enabling the friction and wear of materials in sliding conditions to be compared, it is not wholly representative of the conditions experienced by mechanical seal faces owing to the intermittent nature of the contact. A more realistic simulation is provided by the

thrust-washer test, in which two discs are rotated against each other, which ensures the two surfaces are in continuous contact.

In one early study, that of Hollman et al. [88], diamond-coated WC face seals were compared with a range of other commercially available seal rings, including WC, SiC, Al<sub>2</sub>O<sub>3</sub>, and sintered carbon impregnated with antimony. The test pieces were rings with an inside diameter of 18 mm and outside diameter of 22 mm. The tests were performed in the absence of lubrication at a contact pressure of 2.5 MPa and a sliding velocity of 3.5 m·s<sup>-1</sup>. For CVD diamond sliding against itself, a steady-state coefficient of friction of 0.2 was recorded; for diamond sliding against SiC, it was even lower at 0.1. In contrast, the corresponding figures for self-mated WC and SiC were both in the region of approximately 0.7.

In another study, Kelly et al. [96] used a thrust-washer test to evaluate diamond-coated discs in sliding contact with WC, SiC, or diamond-coated SiC under conditions of marginal water lubrication. The diamond coatings were between 2 and 4 µm in thickness, and the tests were conducted at a sliding speed of 10 mm·s<sup>-1</sup> and a pressure of approximately 0.5 MPa. In tests where both surfaces were diamond-coated, the coefficient of friction was between 0.05 and 0.07. At the conclusion of the test, the coating was intact with only a lightly polished track being visible on both disc and washer. In contrast, in a test of a diamond-coated disc against a SiC washer, rapid coating failure was seen, despite a steady-state coefficient of friction of only 0.05. The reverse was seen in another test combination: a diamond-coated disc against a WC washer. Although the average coefficient of friction was 0.4, the coating on the disc remained intact; however, the measured wear volume in the WC was also approximately 50% higher than that recorded on the SiC.

In a later study, Jones [97] tested a diamond-coated SiC pad against an uncoated SiC cylinder at a velocity of 0.5 m·s<sup>-1</sup>, in this case, without lubrication. The coating was 5–6 µm in thickness, the as-deposited *R*<sub>a</sub> of which was 0.25 µm; no post-deposition treatments such as lapping or polishing were performed. During the tests, the load was increased incrementally until contact instability occurred. The diamond film exhibited an approximately 25-fold improvement in PV capability.

Tome et al. [98] coated Si<sub>3</sub>N<sub>4</sub> rings with diamond coatings of between 8 and 25 µm in thickness; the grain sizes were 2–3.5 µm, while the initial surface roughness values were between 0.15 and 0.26 µm. The rough as-grown surfaces of the diamond films prevented full sealing in the early stages of the ring-on-ring tests, although this was achieved once the asperities were worn down by self-polishing. The coefficient of friction stabilized at approximately 0.05, and remained at this level until the test was stopped. The longest test was conducted for a sliding distance of up to 5700 km with no measurable wear.

Nanocrystalline diamond coatings enable a smooth diamond coating without the need for post-deposition lapping or polishing. This is particularly attractive for applications such as mechanical seals where a low surface roughness is needed to prevent leakages. Mubarok et al. [99] used a ring-on-ring test apparatus to evaluate diamond-coated Si<sub>3</sub>N<sub>4</sub> seals. The nanocrystalline diamond coating (2 µm in thickness) had a surface *R*<sub>a</sub> of 62 nm, which removed the need for running-in procedures. The tests were conducted in a water environment with the sliding speeds between 2 and 4 m·s<sup>-1</sup>, and the loads between 300 and 925 N. With the exception of the highest load/sliding speed combination (925 N/4 m·s<sup>-1</sup>)—in which seizure occurred—the mean steady-state coefficients of friction were between 0.01 and 0.02, while the wear, which was monitored by mass loss, was below the limit of detection. In the case of the test where seizure took place, examination of the sliding surfaces revealed that the diamond coating delaminated from the substrate. The cause of this was ascribed to excessive heating at the contact, which resulted in water vaporization, elimination of the boundary lubrication layer, and removal of the coating.

Sumant et al. [83] evaluated the performance of SiC seals coated with a 2-µm film of ultrananocrystalline diamond (UNCD) running against a carbon counterface in a water pump seal test apparatus. This combination was seen to result in negligible wear for the diamond coating after the test which lasted for 21 days. When tested against a SiC counterface, the UNCD surface recorded low

coefficients of friction ( $\sim 0.04$ ); in contrast, the corresponding figure for uncoated SiC sliding against itself was  $\sim 0.7$ . These differences were also reflected in the differences in the torque measurements for the UNCD seals which were 5–6 times lower than for the SiC/SiC combination. This suggests considerable energy savings may be possible using diamond-coated seals. However, in the UNCD-SiC test, signs of coating delamination were seen after seven days.

A similar study was undertaken by Kovalchenko et al. [100] who tested SiC seals coated with 1- $\mu\text{m}$  UNCD films in a dynamic seal testing facility; the counterface was either uncoated SiC or carbon. Prior to deposition, the seals were polished using 6- $\mu\text{m}$ , 12- $\mu\text{m}$ , or 30- $\mu\text{m}$  diamond powder. After a running-in procedure the tests were conducted at a water pressure of 0.7 MPa for 50 h; the rotation speed was 3600 rpm. Examination of the diamond-coated seals after the tests indicated that the substrates which were polished with the 12- $\mu\text{m}$  and 30- $\mu\text{m}$  diamond powder prior to deposition did not show any measurable wear. Under optical microscopy, the appearances of the wear tracks were not significantly different from the unworn surface. In contrast, for the seals polished with 6- $\mu\text{m}$  diamond powder prior to coating deposition, regions of the coating were removed during the running-in period. Coating failure was seen to occur at the coating-substrate interface.

In 2007, Burgmann Industries GmbH & Co. introduced a diamond-coated mechanical seal for use in multi-phase pumps. A hot-filament CVD process was used to deposit the diamond coating, which was up to 8  $\mu\text{m}$  in thickness. The seal proved to be successful on an abrasive multi-phase pump application in the Canadian oil sands fields [101]. In 2008, another manufacturer, Advanced Diamond Technologies Inc. (ADT), introduced a range of mechanical seals that incorporated UNCD films, which could be run directly against blister-resistant carbon or SiC counterfaces [92]. ADT subsequently introduced a seal that was optimized to withstand fluid loss or dry running in fluid pumps. When run against SiC, the energy dissipation due to friction was seen to reduce by 75% compared with running SiC against itself [102].

Table 3 lists the steady-state coefficients of friction for UNCD-coated seals running against SiC and resin-bonded carbon in the presence of water; for comparison, the corresponding values for SiC against the same counterfaces are also listed [103]. It can be seen that the diamond-coated seals exhibit significantly lower friction than SiC, the benefits of which are twofold: (i) lower energy costs; and (ii) reduced heat generation. Field data indicated that incorporating UNCD-coated seals into pumping systems can deliver reductions in energy usage of up to 5% [104].

**Table 3.** Coefficients of friction of ultrananocrystalline diamond (UNCD)-coated faces running against carbon and SiC, together with the corresponding values for SiC against the same counterfaces [103].

Stationary Ring	Rotating Ring	Coefficient of Friction (in Water)
UNCD	SiC	0.018–0.04
UNCD	Carbon	0.06–0.10
SiC	SiC	>0.18
SiC	Carbon	0.08–0.10

Although they entered commercial service relatively recently, diamond-coated mechanical seals already demonstrated their value in a number of applications. In one oil and gas application, in an environment of water, steam, and sand, a diamond-coated mechanical seal exhibited an operating life of more than 10,000 h [105]. In another setting, Goldschmidt and Gurtler [106] described the use of diamond-coated mechanical seals in pumps used in a pipeline that transports a multi-phase mixture of crude oil, gas, water, and various solids in the Panacocha oilfield in the Amazonian region of Ecuador. The seals are coated with 10- $\mu\text{m}$  diamond, and demonstrated the ability to operate under dry conditions and at temperatures of up to 300 °C. The mixture pumped was also corrosive, owing to the high chloride content in the formation water. Such environments, representing a combination of wear and corrosion, require a multifunctional solution, which can only be met by diamond.

## 5. Control Valves

Approximately 90% of the world's oil and gas wells are drilled in sandstone reservoirs; of these, approximately 25–35% experience some degree of sand production during their productive lives [107]. In general, the sand content in well streams upstream of the first separators is in the range of 1–50 parts per million by mass (ppm w). Typical sand particles are between 100 and 1000  $\mu\text{m}$  if no sand-exclusion techniques are applied; when sand exclusion techniques are employed, typical particle sizes range from 20–200  $\mu\text{m}$  [108]. Figure 9 shows an electron micrograph of a sample of sand obtained from the Forties (North Sea) oilfield. A typical distribution of particle sizes is shown in the histogram in Figure 10.

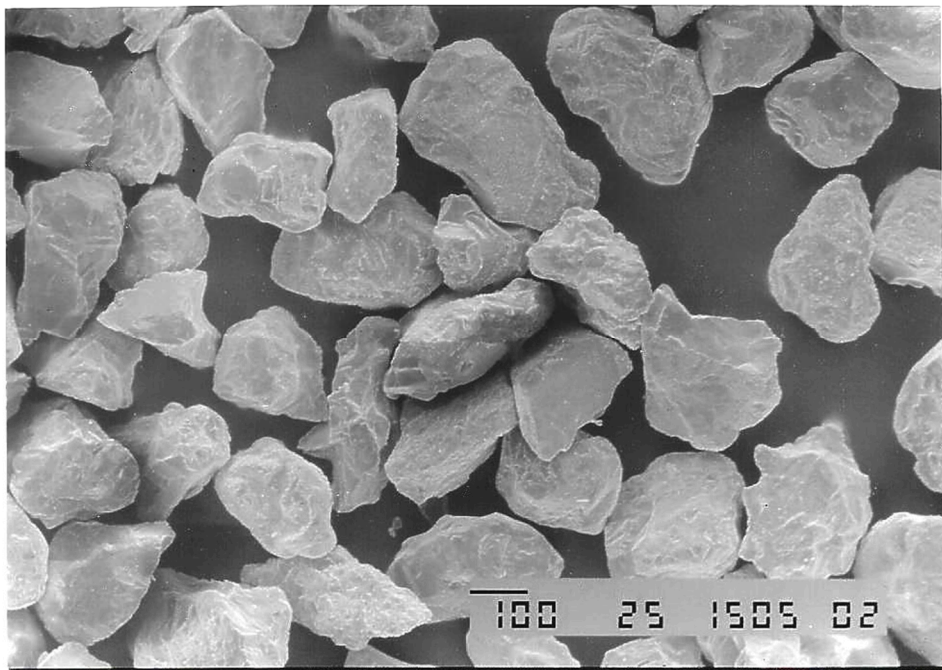


Figure 9. Micrograph of sand from the Forties oilfield.

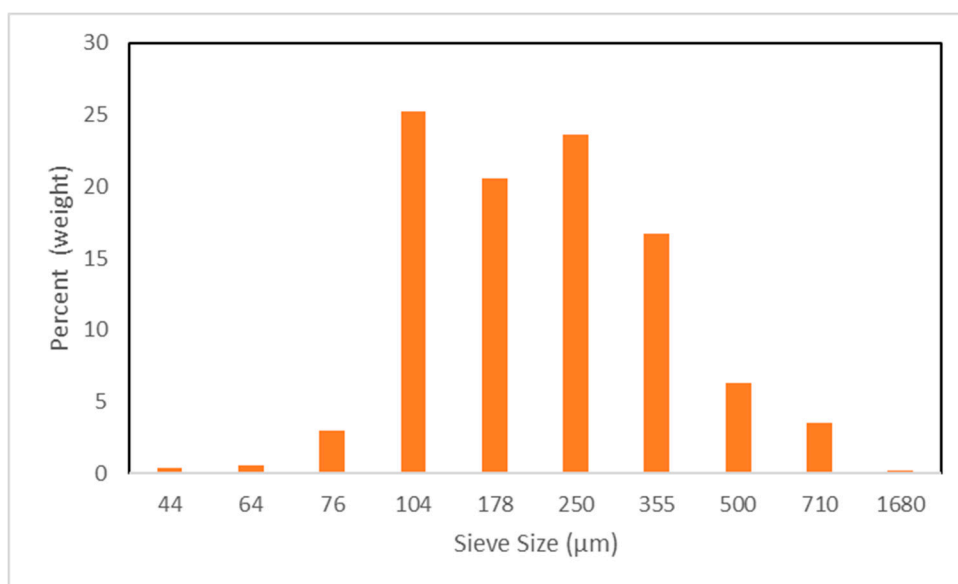


Figure 10. Histogram showing the size distribution of sand from the Forties oilfield.

The presence of sand in the hydrocarbon fluid can result in erosion of valves, pipe bends, and T-junctions. Of these components, erosion is a particular problem for control valves that are used to regulate hydrocarbon fluid flow from the well. In choke valves, which are used to allow the controlled draining of the reservoir, high sand velocities ( $400\text{--}500\text{ m}\cdot\text{s}^{-1}$ ) can be generated when operated at large pressure drops ( $300\text{--}400\text{ bar}$ ) and when the process stream is wholly or partially gaseous. Under these conditions, any sand entrained in the hydrocarbon fluid can cause considerable damage when it impinges on the interior of the valve. According to one survey of 258 failed choke valves, 35% could be attributed to erosion [109].

Choke valves may also be subject to cavitation erosion which can take place downstream of the valve if the local static pressure falls below the fluid vapor pressure. If these bubbles remain in the downstream flow, this can give rise to what is known as “flashing”. The incidence of flashing is more widespread in valves where high pressure drops are generated. However, with correct design and proper sizing of the valve to the flow conditions anticipated, this problem can be minimized.

As well as erosion, abrasion can also be a problem, especially if sand becomes trapped between the sliding surfaces of the valve. Damage as a result of erosion and abrasion can significantly affect valve performance, and lead to its premature withdrawal from service. In extreme cases, in the North Sea, critical components, intended to last 18–24 months, may be completely destroyed within a few weeks, or even hours [110]. In wells where the valves are installed on the seabed rather than on the drilling platforms, the need for the reliable operations of the valves is even more crucial, especially as replacements will impose both extra costs and logistical difficulties. Therefore, there are powerful safety and economic advantages to be derived from extending the operating life of these valves.

One way by which the life of a valve could be extended is by incorporating ultra-hard facings into some of the interior components of the valves to resist erosion from sand particle attack. The most common material used in choke valve trims is cemented WC, accounting for more than 80% according to one survey [111]. However, although its hardness (16 GPa) is greater than that of silica sand (13 GPa) [112], the significantly softer and more ductile Co binder is susceptible to erosion from the sand particles, which leads to loss of the WC grains when the surrounding Co is removed [113]. As a result, the operating life of valves containing WC trim is still only about three years. For this reason, a harder material is required in order to provide enhanced erosion resistance. One such material with the potential to deliver such improvements is diamond.

The solid particle erosion performance of diamond was the subject of numerous studies and from various workers [114–128]. Owing to its high hardness and strength, CVD diamond coatings were shown to exhibit steady-state erosion rates of up to 30 times lower than those of cemented tungsten carbide [118,119,121–123]. Moreover, owing to the greater hardness and fracture toughness of diamond, erosion studies [118] revealed that damage to the impacting sand particles often exceeds that of the coating. However, CVD diamond coatings remain susceptible to catastrophic failure caused by the sub-surface shear stresses generated by the impacting particles if the magnitude of such stresses are sufficient to cause debonding at the coating-substrate interface. A study by Wheeler and Wood [122] found that if the depth of maximum shear stress was sufficiently far removed from the interface, then the life of the coating was limited only by the low rate of micro-chipping that was also caused by the impacting particles.

Laboratory tests have enabled the erosion behavior of diamond coatings to be well understood. In order to evaluate its performance in a choke valve, diamond was also applied to regions of a choke-valve trim and tested under full-scale conditions in a valve loop test facility at the BP Research Center, Sunbury-on-Thames, and compared with standard uncoated WC trims [129]. The valve design used for these tests was the ABB Kent Introl Type 74 (50 mm in diameter), an equal-percentage plug-in-cage design; free-standing CVD diamond, in the form of an annulus approximately 0.6 mm in thickness, was bonded to the end of two WC-6Co plugs and seats using a high-temperature adhesive (see Figures 11 and 12). A water/sand mixture (sand concentration 1% by weight) was recirculated through the valve at a flow rate of  $454\text{ l}\cdot\text{min}^{-1}$  and a pressure drop across the valve of  $60\text{ bar}\cdot\text{g}$ ;

the pressure drop corresponds to a velocity of  $110 \text{ m}\cdot\text{s}^{-1}$ . The sand consisted of a mixture of three commercially available quarry sands blended to reproduce the size distribution found in the Forties oilfield; the mean diameter was  $194 \mu\text{m}$ . The tests were conducted for up to six hours. The results showed that valve seats and plugs with a partial coverage of CVD diamond displayed 50–60% greater resistance to erosion damage caused by sand-particle impingement. The diamond-coated plug had an erosion rate 53% lower than the standard plug. However, the annulus on the plug was partially removed (see Figure 13), not by erosion of the diamond but by erosion of the underlying WC, which led to the diamond becoming debonded along its bond line. It was thought that coating the sides of the plug could reduce the problem of undermining the diamond and further enhance its erosion resistance.



Figure 11. A choke valve plug with a CVD diamond annulus [129].

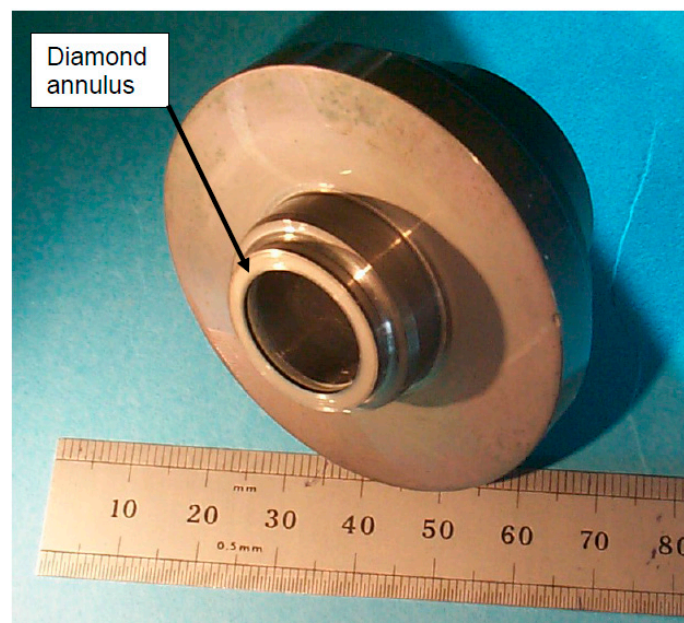
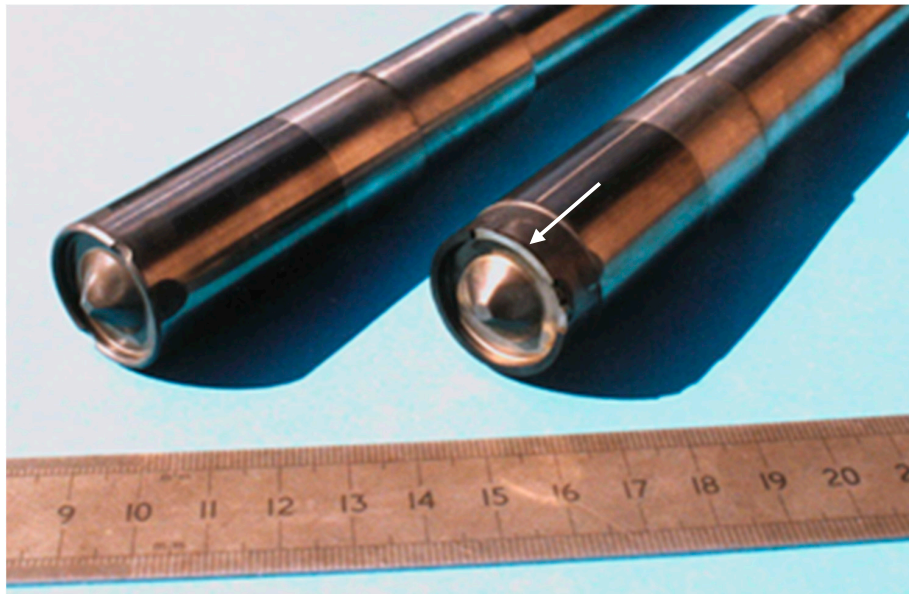


Figure 12. A CVD diamond annulus applied to a choke valve seat [129].



**Figure 13.** Photograph showing a tungsten carbide valve plug (**left**) and a plug containing a diamond annulus (**right**) after testing in a valve loop test facility for 6 h. The arrow indicates the region where the diamond annulus was removed.

In the case of the valve seat, it was found that bonding diamond to the central rim of the seat reduced the magnitude of the erosion; the erosion rate of the diamond-coated seat was 60% lower than the standard design. The diamond was essentially undamaged. This contrasted with the WC seat, which exhibited notable rounding during the test (see Figure 14). Overall, however, the extent of erosion of both seats was lower than the plugs of the same material.



**Figure 14.** Photograph showing a tungsten carbide valve seat (**left**) and a seat containing a diamond annulus (**right**) after testing in a valve loop test facility for six hours. It is worth noting that the diamond annulus prevented rounding of the inner rim, which can be seen on the tungsten carbide seat.

The erosion rates of the valve cages were the highest of the three trim components. However, they were not coated with diamond because of the difficulties presented by the complex geometry of this component. The cage was of a two-stage design with the inner cage suffering the greatest damage

with a number of deep scars on its outer surface. The eroded inner and outer cage can be seen in Figure 15. The appearance of the inner cage suggested that a diamond coating on the outer surface of this component could greatly reduce cage wear. However, there are significant difficulties associated with carrying out such a task. The deposition of diamond films onto some non-planar substrates remains a formidable challenge.

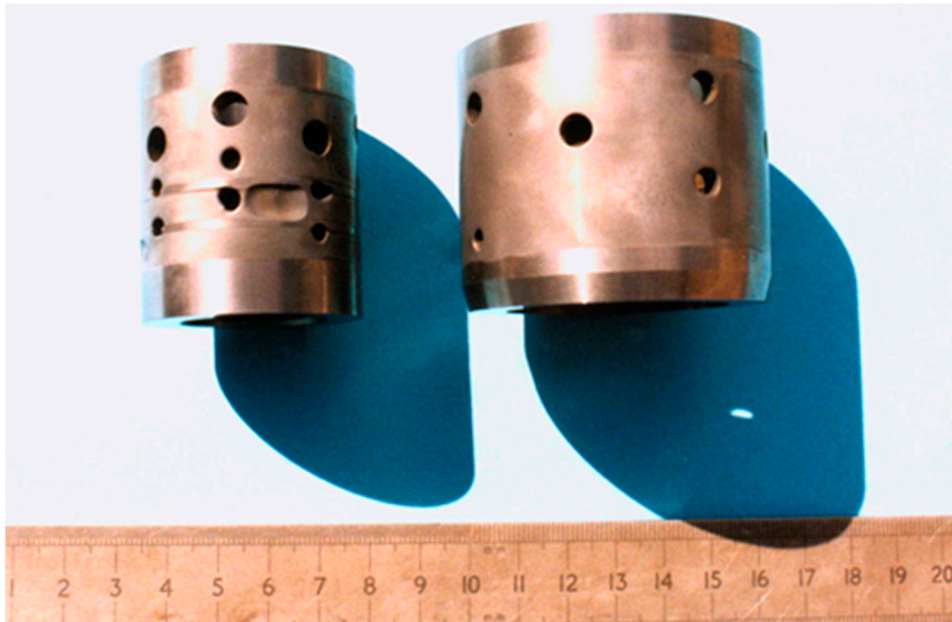


**Figure 15.** Photograph of the two parts of a tungsten-carbide valve cage tested for 6 h in a valve loop test facility showing typical erosion damage, particularly on the inner cage (left).

## 6. Conclusions

Diamond is shown to offer considerable improvements to the operating lives of components used in the oil and gas industry, with benefits ranging from reduced operating and maintenance costs to improved productivity. Although the initial costs of the diamond-containing components can be significantly greater than those of non-diamond alternatives, the extra costs can be more than outweighed by the increased efficiencies.

In drilling applications, high abrasion resistance enables PDC cutters to stay sharp for longer, resulting in longer bit lives, even in highly abrasive rock formations [58]. Indeed, in some cases, it is not uncommon for a single PDC bit to drill more than 2500 m [51]. Research into drilling materials yielded sizeable financial gains, as demonstrated by one particular research and development (R&D) program on PDC drill bits, in which the economic benefits (e.g., net manufacturing profits and drill cost savings) were estimated to be \$125 for every dollar invested [130].

Diamond-coated mechanical seals have the potential to deliver significant cost savings to plant operators. According to one estimate, for a petrochemical plant operating 1200 pumps, a 25% increase in mean time between failures (MTBF) could result in an annual saving of up to \$1.8 million in maintenance costs [104].

The high wear resistance and low friction behavior of diamond were shown to deliver extended operating lives and reduced friction losses (and hence, reduced energy consumption) in diamond-coated mechanical seals. In one example, an uncoated SiC seal operating for 8000 hours per year converted 3200 kWh into friction; this figure was reduced by approximately 2500 kWh over the same period when it was coated with diamond. This saving translated into approximately €325 in industrial electricity prices [131]. Furthermore, analyses have shown that the return on investment due to the significantly improved service life achieved by a diamond-coated mechanical seal can be obtained after just 18 months [132].

**Funding:** This research received no external funding.

**Acknowledgments:** The author would like to thank Element Six (UK) Ltd. (Harwell, Oxfordshire, UK) for granting permission to use the images in Figure 3, Figure 5, and Figure 6, and J. Pickles for reading and commenting on the manuscript in draft form. The content and opinions in this article are those of the author alone and are not the views of AWE plc or any of its partners or the UK Government.

**Conflicts of Interest:** The author declares no conflict of interest.

## References

1. Papavinasan, S. *Corrosion Control in the Oil and Gas Industry*; Gulf Professional Publishing: London, UK, 2014.
2. Wheeler, D.W. CVD diamond: A multifunctional tribological material. In *Multifunctional Materials for Tribological Applications*; Wood, R.J.K., Ed.; Pan Stanford Publishing Pte. Ltd.: Singapore, 2015; pp. 1–58.
3. Scott, T.A. The influence of microstructure on the mechanical properties of polycrystalline diamond: A literature review. *Adv. Appl. Ceram.* **2018**, *117*, 161–176. [[CrossRef](#)]
4. Walmsley, J.C.; Lang, A.R. Characteristics of diamond regrowth in a synthetic diamond compact. *J. Mater. Sci.* **1988**, *23*, 1829–1834. [[CrossRef](#)]
5. Lammer, A. Mechanical properties of polycrystalline diamonds. *Mater. Sci. Technol.* **1988**, *4*, 949–955. [[CrossRef](#)]
6. Bruton, G.; Crockett, R.; Taylor, M.; DenBoer, D.; Lund, J.; Fleming, C.; Ford, R.; Garcia, G.; White, A. PDC bit technology for the 21st century. *Oilfield Rev.* **2014**, *26*, 48–57.
7. Wilks, J.; Wilks, E. *Properties and Applications of Diamond*; Butterworth Heinemann: Oxford, UK, 1991.
8. Mehan, R.L.; Hibbs, L.E. Thermal degradation of sintered diamond compacts. *J. Mater. Sci.* **1989**, *24*, 942–950. [[CrossRef](#)]
9. Liu, C.; Kou, Z.; He, D.; Chen, Y.; Wang, K.; Hui, B.; Zheng, R.; Wang, Y. Effect of removing internal residual metallic phases on wear resistance of polycrystalline diamond compacts. *Int. J. Refract. Met. Hard Mater.* **2012**, *31*, 187–191. [[CrossRef](#)]
10. Boland, J.N.; Li, X.S. Microstructural characterisation and wear behaviour of diamond composite materials. *Materials* **2010**, *3*, 1390–1419. [[CrossRef](#)]
11. May, P.W. Diamond thin films: A 21st century material. *Philos. Trans. R. Soc. Lond. A* **2000**, *358*, 473–495. [[CrossRef](#)]
12. Yan, G.; Yue, W.; Meng, D.; Lin, F.; Wu, Z.; Wang, C. Wear performance and mechanisms of ultrahard polycrystalline diamond composite material grinded against granite. *Int. J. Refract. Met. Hard Mater.* **2016**, *54*, 46–53. [[CrossRef](#)]
13. Field, J.E. The mechanical and strength properties of diamond. *Rep. Prog. Phys.* **2012**, *75*, 126505. [[CrossRef](#)] [[PubMed](#)]
14. Jianxin, D.; Hui, Z.; Ze, W.; Aihua, L. Friction and wear behaviour of polycrystalline diamond at temperatures up to 700 °C. *Int. J. Refract. Met. Hard Mater.* **2011**, *29*, 631–638. [[CrossRef](#)]
15. Hess, P. The mechanical properties of various chemical vapor deposition diamond structures compared to the ideal single crystal. *J. Appl. Phys.* **2012**, *111*, 051101. [[CrossRef](#)]
16. Telling, R.H.; Field, J.E. The erosion of diamond, sapphire and zinc sulphide by quartz particles. *Wear* **1999**, *233–235*, 666–673. [[CrossRef](#)]
17. Drory, M.D.; Dauskardt, R.H.; Kant, A.; Ritchie, R.O. Fracture of synthetic diamond. *J. Appl. Phys.* **1995**, *78*, 3083–3088. [[CrossRef](#)]
18. Sussmann, R.S.; Brandon, J.R.; Scarsbrook, G.A.; Sweeney, C.G.; Valentine, T.J.; Whitehead, A.J.; Wort, C.J.H. Properties of bulk polycrystalline CVD diamond. *Diamond Relat. Mater.* **1994**, *3*, 303–312. [[CrossRef](#)]
19. Davies, A.R.; Field, J.E.; Pickles, C.S.J. Strength of free-standing chemically vapour-deposited diamond measured by a range of techniques. *Philos. Mag.* **2003**, *83*, 4059–4070. [[CrossRef](#)]
20. Field, J.E. *The Properties of Natural and Synthetic Diamond*; Academic Press: London, UK, 1992.
21. Twitchen, D.J.; Pickles, C.S.J.; Coe, S.E.; Sussmann, R.S.; Hall, C.E. Thermal conductivity measurements on CVD diamond. *Diamond Relat. Mater.* **2001**, *10*, 731–735. [[CrossRef](#)]
22. Wort, C.J.H.; Sweeney, C.G.; Cooper, M.A.; Scarsbrook, G.A.; Sussmann, R.S. Thermal properties of bulk polycrystalline CVD diamond. *Diamond Relat. Mater.* **1994**, *3*, 1158–1167. [[CrossRef](#)]
23. Boart Longyear. *Data Sheets for Tungsten Carbide Grades*; Boart Longyear: Salt Lake City, UT, USA, 1998.

24. Beste, U. On the Nature of Cemented Carbide Wear in Rock Drilling. Ph.D. Thesis, University of Uppsala, Uppsala, Sweden, 2004.
25. Mpagazehe, J.N.; Queiruga, A.F.; Higgs, C.F. Towards an understanding of the drilling process for fossil fuel energy: A continuum-discrete approach. *Tribol. Int.* **2013**, *59*, 273–283. [[CrossRef](#)]
26. Macdonald, K.A.; Bjune, J.V. Failure analysis of drillstrings. *Eng. Fail. Anal.* **2007**, *14*, 1641–1666. [[CrossRef](#)]
27. Beste, U.; Jacobson, S. Micro scale hardness distribution of rock types related to rock drill wear. *Wear* **2003**, *254*, 1147–1154. [[CrossRef](#)]
28. Bobko, C.; Ulm, F.J. The nano-mechanical morphology of shale. *Mech. Mater.* **2008**, *40*, 318–337. [[CrossRef](#)]
29. Zhu, W.; Hughes, J.J.; Bicanic, N.; Pearce, C.J. Nanoindentation mapping of mechanical properties of cement paste and natural rocks. *Mater. Charact.* **2007**, *58*, 1189–1198. [[CrossRef](#)]
30. Shukla, P.; Kumar, V.; Curtis, M.; Sondergeld, C.H.; Rai, C.S. Nanoindentation studies on shales. Presented at 47th US Rock Mechanics/Geomechanics Symposium, San Francisco, CA, USA, 23–26 June 2013.
31. Eliyahu, M.; Emmanuel, S.; Day-Stirrat, R.J.; Macaulay, C.I. Mechanical properties of organic matter in shales mapped at the nanometer scale. *Mar. Petrol. Geol.* **2015**, *59*, 294–304. [[CrossRef](#)]
32. Liu, K.; Ostadhassan, M.; Bubach, B. Applications of nano-indentation methods to estimate nanoscale mechanical properties of shale reservoir rocks. *J. Nat. Gas Sci. Eng.* **2016**, *35*, 1310–1319. [[CrossRef](#)]
33. Liu, K.; Ostadhassan, M. Microstructural and geomechanical analysis of Bakken shale at nanoscale. *J. Petrol. Sci. Eng.* **2017**, *153*, 133–144. [[CrossRef](#)]
34. Liu, K.; Ostadhassan, M.; Bubach, B.; Ling, K.; Tokhmechi, B.; Robert, D. Statistical grid nanoindentation analysis to estimate macro-mechanical properties of the Bakken shale. *J. Nat. Gas Sci. Eng.* **2018**, *53*, 181–190. [[CrossRef](#)]
35. Heinrichs, J.; Olsson, M.; Jacobson, S. Surface degradation of cemented carbides in scratching contact with granite and diamond—the roles of microstructure and composition. *Wear* **2015**, *342–343*, 210–221. [[CrossRef](#)]
36. Han, Q.; Chen, P.; Ma, T. Influencing factor analysis of shale micro-indentation measurement. *J. Nat. Gas Sci. Eng.* **2015**, *27*, 641–650. [[CrossRef](#)]
37. Chen, P.; Han, Q.; Ma, T.; Lin, D. The mechanical properties of shale based on micro-indentation test. *Petrol. Explor. Dev.* **2015**, *42*, 723–732. [[CrossRef](#)]
38. Cala, M.; Cyran, K.; Kawa, M.; Kolano, M.; Lydzba, D.; Pachnicz, M.; Rajczakowska, M.; Rozanski, A.; Sobotka, M.; Stefaniuk, D.; et al. Identification of microstructural properties of shale by combined use of X-ray micro-CT and nanoindentation tests. *Procedia Eng.* **2017**, *191*, 735–743. [[CrossRef](#)]
39. Veytskin, Y.B.; Tammina, V.K.; Bobko, C.P.; Hartley, P.G.; Clennell, M.B.; Dewhurst, D.N.; Dagastine, R.R. Micromechanical characterisation of shales through nanoindentation and energy dispersive X-ray spectrometry. *Geomech. Energy Environ.* **2017**, *9*, 21–35. [[CrossRef](#)]
40. Scott, D.E. The History And Impact of Synthetic Diamond Cutters and Diamond Enhanced Inserts on the Oil and Gas Industry. Available online: [http://pdc-guru.com/uploads/2/8/7/9/2879895/daw\\_d-scott\\_history-and-impact-of-synthetic-diamond-cutters-in-og.pdf](http://pdc-guru.com/uploads/2/8/7/9/2879895/daw_d-scott_history-and-impact-of-synthetic-diamond-cutters-in-og.pdf) (accessed on 19 January 2018).
41. Jamison, W.E. Tools for rock drilling. In *Wear Control Handbook*; Peterson, M.B., Winer, W.O., Eds.; American Society of Mechanical Engineers: New York, NY, USA, 1980; pp. 859–890.
42. Petrica, M.; Badisch, E.; Peinsitt, T. Abrasive wear mechanisms and their relation to rock properties. *Wear* **2013**, *308*, 86–94. [[CrossRef](#)]
43. Belozarov, D. Drill Bits Optimization in the Eldfisk Overburden. Master's Thesis, University of Stavanger, Stavanger, Norway, 2015. Available online: [https://brage.bibsys.no/xmlui/bitstream/handle/11250/301097/Belozarov\\_Dmitriy.pdf?sequence=1&isAllowed=y](https://brage.bibsys.no/xmlui/bitstream/handle/11250/301097/Belozarov_Dmitriy.pdf?sequence=1&isAllowed=y) (accessed on 8 April 2018).
44. Azar, M.; Long, W.; White, A.; Copeland, C.; Hempton, R.; Pak, M. A new approach to fixed cutter bits. *Oilfield Rev.* **2015**, *27*, 30–35.
45. Torrance, A.A. Modelling abrasive wear. *Wear* **2005**, *258*, 281–293. [[CrossRef](#)]
46. Misra, A.; Finnie, I.M. An experimental study of three-body abrasive wear. *Wear* **1983**, *85*, 57–68. [[CrossRef](#)]
47. Gerk, C.; Yan-Gerk, L.; Wesling, V.; Reiter, R. Highly carbide filled composite materials for the mining and drilling industry. *IOP Conf. Ser.: Mater. Sci. Eng.* **2016**, *118*, 012011. [[CrossRef](#)]
48. Albdiry, M.T.; Almensory, M.F. Failure analysis of drillstring in petroleum industry: A review. *Eng. Fail. Anal.* **2016**, *65*, 74–85. [[CrossRef](#)]

49. Glowka, D. Development of a Method for Predicting the Performance and Wear of PDC Drill Bits. Sandia National Laboratory Report SAND-86-1745; 1987. Available online: <http://prod.sandia.gov/techlib/access-control.cgi/1986/861745.pdf> (accessed on 2 April 2018).
50. Coomber, N. Diamond Drilling Shows its Sparkle. Available online: <https://www.offshore-technology.com/features/feature63772/> (accessed on 8 April 2018).
51. Roller Cones vs. Diamonds: A Reversal of Roles. *Oil and Gas Journal* 2/20/2006. Available online: <https://www.ogj.com/articles/print/volume-104/issue-7/supplement-to-oil-gas-journal/advances-in-drill-bit-technology/roller-cones-vs-diamonds-a-reversal-of-roles.html> (accessed on 8 April 2018).
52. Yahiaoui, M.; Gerbaud, L.; Paris, J.-Y.; Denape, J.; Dourfaye, A. A study on PDC drill bits quality. *Wear* **2013**, *298–299*, 32–41. [[CrossRef](#)]
53. Menand, S.; Gerbaud, L.; Dourfaye, A. *PDC Bit Technology Improvements Increase Efficiency, Bit Life*; Drilling Contractor: Houston, TX, USA, March/April 2005; pp. 52–54.
54. Che, D.; Zhu, W.-L.; Ehmann, K.F. Chipping and crushing mechanisms in orthogonal rock cutting. *Int. J. Mech. Sci.* **2016**, *119*, 224–236. [[CrossRef](#)]
55. Che, D.; Ehmann, K. Experimental study of force responses in polycrystalline diamond face turning of rock. *Int. J. Rock Mech. Min. Sci.* **2014**, *72*, 80–91. [[CrossRef](#)]
56. Geoffroy, H.; Minh, D.N.; Maitournam, H.; Bergues, J.; Putot, C. Evaluation of drilling parameters of a PDC bit. In *Advances in Rock Mechanics*; Lin, Y., Ed.; World Scientific Publishing Co. Pte. Ptd.: Singapore, 1998; pp. 301–314.
57. Wamsley, W.H., Jr.; Ford, R. Introduction to Roller-Cone and Polycrystalline Diamond Drill Bits. In *Petroleum Engineering Handbook, Vol II: Drilling Engineering*; Lake, L.W., Ed.; Society of Petroleum Engineers: Richardson, TX, USA, 2006; pp. 221–264.
58. Clark, I.E.; Bex, P.A. The use of PCD for petroleum and mining drilling. *Ind. Diamond Rev.* **1999**, *59*, 43–49.
59. Williams, J.L.; Thompson, A.I. An Analysis of the Performance of PDC Hybrid Drill Bits. In Proceedings of the SPE/IADC Drilling Conference, New Orleans, LA, USA, 15–18 March 1987; Society of Petroleum Engineers: Richardson, TX, USA, 1997.
60. Dougherty, P.S.M.; Pudjoprawoto, R.; Higgs, C.F., III. Bit cutter-on-rock tribometry: Analysing friction and rate-of-penetration for deep well drilling substrates. *Tribol. Int.* **2014**, *77*, 178–185. [[CrossRef](#)]
61. Dougherty, P.S.M.; Mpagazehe, J.; Shelton, J.; Higgs, C.F., III. Elucidating PDC rock cutting behaviour in dry and aqueous conditions using tribometry. *J. Petrol. Sci. Eng.* **2015**, *133*, 529–542. [[CrossRef](#)]
62. Dagrain, F.; Richard, T. On the influence of PDC wear and rock type on friction coefficient and cutting efficiency. In *Eurock 2006: Multiphysics Coupling and Long Term Behaviour in Rock Mechanics*; CRC Press: Boca Raton, FL, USA, 2006; pp. 577–584.
63. Ersoy, A.; Waller, M.D. Wear characteristics of PDC in and hybrid core bits in rock drilling. *Wear* **1995**, *188*, 150–165. [[CrossRef](#)]
64. Abbas, R.K. A review on the wear of oil drill bits (conventional and the state of the art approaches for wear reduction and quantification). *Eng. Fail. Anal.* **2018**, *90*, 554–584. [[CrossRef](#)]
65. Yahiaoui, M.; Paris, J.-Y.; Delbe, K.; Denape, J.; Gerbaud, L.; Dourfaye, A. Independent analyses of cutting and friction forces applied on a single polycrystalline diamond compact cutter. *Int. J. Rock Mech. Min. Sci.* **2016**, *85*, 20–26. [[CrossRef](#)]
66. Gant, A.J.; Konyashin, I.; Ries, B.; McKie, A.; Nilen, R.W.N.; Pickles, J. Wear mechanisms of diamond-containing hardmetals in comparison with diamond-based materials. *Int. J. Refract. Met. Hard Mater.* **2018**, *71*, 106–114. [[CrossRef](#)]
67. Miess, D.; Rai, G. Fracture toughness and thermal resistance of polycrystalline diamond compacts. *Mater. Sci. Eng. A* **1996**, *209*, 270–276. [[CrossRef](#)]
68. Yahiaoui, M.; Paris, J.-Y.; Delbe, K.; Denape, J.; Gerbaud, L.; Colin, C.; Ther, O.; Dourfaye, A. Quality and wear behaviour of graded polycrystalline diamond compact cutters. *Int. J. Refract. Met. Hard Mater.* **2016**, *56*, 87–95. [[CrossRef](#)]
69. Kanyanta, V.; Dormer, A.; Murphy, N.; Invankovic, A. Impact fatigue fracture of polycrystalline diamond compact (PDC) cutters and the effect of microstructure. *Int. J. Refract. Met. Hard Mater.* **2014**, *46*, 145–151. [[CrossRef](#)]
70. Garcia-Marro, F.; Mestra, A.; Kanyanta, V.; Maweja, K.; Ozbayraktar, S.; Llanes, L. Contact damage and residual strength in polycrystalline diamond (PCD). *Diamond Relat. Mater.* **2016**, *65*, 131–136. [[CrossRef](#)]

71. Westraadt, J.E.; Sigalas, I.; Neethling, J.H. Characterisation of thermally degraded polycrystalline diamond. *Int. J. Refract. Met. Hard Mater.* **2015**, *48*, 286–292. [[CrossRef](#)]
72. Miyazaki, K.; Ohno, T.; Karasawa, H.; Takahura, S.; Eko, A. Performance evaluation of polycrystalline diamond compact percussion bits through drilling tests. *Int. J. Rock Mech. Min. Sci.* **2016**, *87*, 1–7. [[CrossRef](#)]
73. Bellin, F.; Dourfaye, A.; King, W.; Thigpen, M. *The Current State of PDC Bit Technology. Part 1*; World Oil: Houston, TX, USA, September 2010; pp. 41–46.
74. Bellin, F.; Dourfaye, A.; King, W.; Thigpen, M. *The Current State of PDC Bit Technology. Part 3*; World Oil: Houston, TX, USA, November 2010; pp. 67–71.
75. Field, J.E.; Pickles, C.S.J. Strength, fracture and friction properties of diamond. *Diamond Relat. Mater.* **1996**, *5*, 625–634. [[CrossRef](#)]
76. Nagel, D.D. Well Drilling Tool with Diamond Thrust Bearings. U.S. Patent 4,620,601, 4 November 1986.
77. Knuteson, C.W.; Sexton, T.N.; Cooley, C.H. Wear-in behaviour of polycrystalline diamond thrust bearings. *Wear* **2011**, *271*, 2106–2110. [[CrossRef](#)]
78. Geczy, B.A. Thrust Bearing Assembly for a Downhole Drill Motor. U.S. Patent 4,560,014, 24 December 1985.
79. Sexton, T.N.; Cooley, C.H. Polycrystalline diamond thrust bearings for down-hole oil and gas drilling tools. *Wear* **2009**, *267*, 1041–1045. [[CrossRef](#)]
80. Ide, R.C. Hydrodynamic thrust bearings for downhole mud motor use. Presented at American Association of Drilling Engineers National Technical Conference and Exhibition, Houston, TX, USA, 12–14 April 2011.
81. Hayward, I.P.; Singer, I.L.; Seitzman, L.E. Effect of roughness on the friction of diamond on CVD diamond coatings. *Wear* **1992**, *157*, 215–227. [[CrossRef](#)]
82. Bull, S.J.; Chalker, P.R.; Johnston, C.; Moore, V. The effect of roughness on the friction and wear of diamond thin films. *Surf. Coat. Technol.* **1994**, *68–69*, 603–610. [[CrossRef](#)]
83. Sumant, A.V.; Krauss, A.R.; Gruen, D.M.; Auciello, O.; Erdemir, A.; Williams, M.; Artiles, A.F.; Adams, W. Ultrananocrystalline diamond film as a wear-resistant and protective coating for mechanical seal applications. *Tribol. Trans.* **2005**, *48*, 24–31. [[CrossRef](#)]
84. Abreu, C.S.; Oliviera, F.J.; Belmonte, M.; Fernandes, A.J.S.; Silva, R.F.; Gomes, J.R. Grain size effect on self-mated CVD diamond tribosystems. *Wear* **2005**, *259*, 771–778. [[CrossRef](#)]
85. Abreu, C.S.; Amaral, M.; Fernandes, A.J.S.; Oliviera, F.J.; Silva, R.F.; Gomes, J.R. Friction and wear performance of HFCVD nanocrystalline diamond coated silicon nitride ceramics. *Diamond Relat. Mater.* **2006**, *15*, 739–744. [[CrossRef](#)]
86. Schade, A.; Rosiwal, S.M.; Singer, R.F. Influence of surface topography of HF-CVD diamond films on self-mated planar sliding contacts in dry environments. *Surf. Coat. Technol.* **2007**, *201*, 6197–6205. [[CrossRef](#)]
87. Abreu, C.S.; Salgueiredo, E.; Oliviera, F.J.; Fernandes, A.J.S.; Silva, R.F.; Gomes, J.R. CVD diamond water lubricated tribosystems for high load planar sliding. *Wear* **2008**, *265*, 1023–1028. [[CrossRef](#)]
88. Hollman, P.; Bjorkman, H.; Alahelisten, A.; Hogmark, S. Diamond coatings applied to mechanical face seals. *Surf. Coat. Technol.* **1998**, *105*, 169–174. [[CrossRef](#)]
89. Neale, M.J. *The Tribology Handbook*, 2nd ed.; Butterworth-Heinemann: Oxford, UK, 1995.
90. Parrott, S. Engineering ceramics for aggressive environments. *Mat. Mater.* **1990**, *6*, 207–210.
91. Nau, B.S. Mechanical seal face materials. *Proc. Inst. Mech. Eng. Part J J. Eng. Tribol.* **1997**, *211*, 165–183. [[CrossRef](#)]
92. Diamond pump seals launched. *Seal. Technol.* **2008**, *2008*, 1. [[CrossRef](#)]
93. Zou, M.; Green, I. Real-time condition monitoring of mechanical face seal. In *Tribology for Energy Conservation*; Dowson, D., Taylor, C.M., Childs, T.H.C., Dalmaz, G., Berthier, Y., Flamand, L., Georges, J.M., Lubrecht, A., Eds.; Elsevier Science B.V.: Amsterdam, The Netherlands, 1998; pp. 423–430.
94. Jones, G.A. On the tribological behaviour of mechanical seal face materials in dry line contact Part I. Mechanical carbon. *Wear* **2004**, *256*, 415–432. [[CrossRef](#)]
95. Thorvart, L. The materials key to seal performance. *Mater. World* **1994**, *2*, 519–521.
96. Kelly, P.J.; Arnell, R.D.; Hudson, M.D.; Wilson, A.E.J.; Jones, G. Enhanced mechanical seal performance through CVD diamond films. *Vacuum* **2001**, *61*, 61–74. [[CrossRef](#)]
97. Jones, G.A. On the tribological behaviour of mechanical seal face materials in dry line contact Part II. Bulk ceramics, diamond and diamond-like carbon films. *Wear* **2004**, *256*, 433–455. [[CrossRef](#)]
98. Tome, M.A.; Fernandes, A.J.S.; Oliveira, F.J.; Silva, R.F.; Carrapichano, J.M. High performance sealing with CVD diamond self-mated rings. *Diamond Relat. Mater.* **2005**, *14*, 617–621. [[CrossRef](#)]

99. Mubarok, F.; Carrapichano, J.M.; Almeida, F.A.; Fernandes, A.J.S.; Silva, R.F. Enhanced sealing performance with CVD nanocrystalline diamond films in self-mated mechanical seals. *Diamond Relat. Mater.* **2008**, *17*, 1132–1136. [CrossRef]
100. Kovalchenko, A.M.; Elam, J.W.; Erdemir, A.; Carlisle, J.A.; Auciello, O.; Libera, J.A.; Pellin, M.J.; Gruen, D.M.; Hryn, J.N. Development of ultrananocrystalline diamond (UNCD) coatings for multipurpose mechanical pump seals. *Wear* **2011**, *270*, 325–331. [CrossRef]
101. Diamond faces deliver performance. *Seal. Technol.* **2007**, *2007*, 2–3. [CrossRef]
102. Diamond wear surfaces optimized for dry running. *Seal. Technol.* **2010**, *2010*, 16. [CrossRef]
103. *UNCD Faces Technical Information*; Advanced Diamond Technologies, Inc.: Romeoville, IL, USA, 2018.
104. *Diamond Coatings for Industrial Components*; Advanced Diamond Technologies Inc.: Romeoville, IL, USA, 2018; Available online: <http://www.thindiamond.com/wp-content/uploads/2018/04/148732-FINAL-ADT-BROCHURE-RA-vs4.pdf> (accessed on 19 June 2018).
105. Otschik, J.; Schrufer, A.; Thelke, J.; Kirchhof, M.; Schmaderer, S. Diamond seal faces—The benefits. *World Pumps* **2010**, 18–20. [CrossRef]
106. Goldschmidt, A.; Gurtler, T. DiamondFace-coated seals ensure pumps run smoothly at remote field in Ecuador. *Seal. Technol.* **2013**, 10–11. [CrossRef]
107. Walton, I.C.; Atwood, D.C.; Halleck, P.M.; Bianco, L.C.B. Perforating unconsolidated sands: An experimental and theoretical investigation. *SPE Drill. Complet.* **2002**, *17*, 141–150. [CrossRef]
108. *Recommended Practice: Managing Sand Production and Erosion*; DNV Report DNVGL-RP-0501; DNV GL: Høvik, Norway, August 2015.
109. Forder, A.F.; Thew, M.T.; Harrison, D. The erosion of oilfield control valves by turbulent particulate suspensions. In Proceedings of the 2nd International Conference Valves, Actuators and Systems: Problems and Solutions, Cambridge, UK, 14–15 April 1997; Blanford, G., Ed.; Independent Technical Conferences, Bedford. 1997; pp. 191–204.
110. Haugen, K.; Kvernfold, O.; Ronold, A.; Sandberg, R. Sand erosion of wear-resistant material: Erosion in choke valves. *Wear* **1995**, *186–187*, 179–188. [CrossRef]
111. Wood, R.J.K.; Wheeler, D.W. Erosion of candidate hard surface coatings for valve applications. In Proceedings of the 2nd International Conference Valves, Actuators and Systems: Problems and Solutions, Cambridge, UK, 14–15 April 1997; Blanford, G., Ed.; Independent Technical Conferences, Bedford. 1997; pp. 217–224.
112. Shipway, P.H.; Hutchings, I.M. The role of particle properties in the erosion of brittle materials. *Wear* **1996**, *193*, 105–113. [CrossRef]
113. Pennefather, R.C.; Hankey, S.E.; Hutchings, R.; Ball, A. Recent observations of the erosion of hard materials. *Mater. Sci. Eng. A* **1988**, *105–106*, 389–394. [CrossRef]
114. Feng, Z.; Tzeng, Y.; Field, J.E. Solid particle impact of CVD diamond films. *Thin Solid Films* **1992**, *212*, 35–42. [CrossRef]
115. Jilbert, G.H.; Pickles, C.S.J.; Coad, E.J.; Field, J.E. Diamond: An erosion resistant aerospace material. In *Applications of Diamond Films and Related Materials: 3rd International Conference*; National Institute of Standards and Technology: Gaithersburg, MD, USA, 1995; pp. 561–564.
116. Davies, A.R.; Field, J.E. The solid particle erosion of free-standing CVD diamond. *Wear* **2002**, *252*, 96–102. [CrossRef]
117. Telling, R.H.; Field, J.E. Fracture and erosion of CVD diamond. *Diamond Relat. Mater.* **1999**, *8*, 850–854. [CrossRef]
118. Wheeler, D.W.; Wood, R.J.K. Erosive wear behaviour of thick chemical vapour deposited diamond coatings. *Wear* **1999**, *225–229*, 523–536. [CrossRef]
119. Wheeler, D.W.; Wood, R.J.K. Solid particle erosion of CVD diamond coatings. *Wear* **1999**, *233–235*, 306–318. [CrossRef]
120. Wheeler, D.W.; Wood, R.J.K. Solid particle erosion of diamond coatings under non-normal impact angles. *Wear* **2001**, *250*, 795–801. [CrossRef]
121. Wheeler, D.W.; Wood, R.J.K. CVD diamond: Erosion-resistant hard material. *Surf. Eng.* **2003**, *19*, 466–470. [CrossRef]
122. Wheeler, D.W.; Wood, R.J.K. Erosion damage in diamond coatings by high velocity sand impacts. *Philos. Mag.* **2007**, *87*, 5719–5740. [CrossRef]

123. Wheeler, D.W.; Wood, R.J.K. Fracture of diamond coatings by high velocity sand erosion. *Philos. Mag.* **2009**, *89*, 285–310. [[CrossRef](#)]
124. Lu, F.X.; He, Q.; Guo, S.B.; Zhang, F.L.; Tong, Y.M. Sand erosion of freestanding diamond films prepared by DC arcjet. *Diamond Relat. Mater.* **2010**, *19*, 936–941. [[CrossRef](#)]
125. Almeida, F.A.; Derkaoui, N.; Oliveira, F.J.; Benedic, F.; Silva, R.F.; Gicquel, A. Erosive wear resistance of NCD coatings produced by pulsed microwave discharges. *Diamond Relat. Mater.* **2010**, *19*, 484–488. [[CrossRef](#)]
126. Wang, X.; Zhang, J.; Shen, B.; Zhang, T.; Sun, F. Erosion mechanism of the boron-doped diamond films of different thicknesses. *Wear* **2014**, *312*, 1–10. [[CrossRef](#)]
127. Wang, X.; Zhang, J.; Shen, B.; Zhang, T.; Sun, F. Fracture and solid particle erosion of micro-crystalline, nano-crystalline and boron-doped diamond films. *Int. J. Refract. Met. Hard Mater.* **2014**, *45*, 31–40. [[CrossRef](#)]
128. Wang, X.; Shen, X.; Sun, F.; Shen, B. Mechanical properties and solid particle erosion of MCD films synthesized using different carbon sources by BE-HFCVD. *Int. J. Refract. Met. Hard Mater.* **2016**, *54*, 370–377. [[CrossRef](#)]
129. Wheeler, D.W.; Wood, R.J.K.; Harrison, D.; Smith, E. Application of diamond to enhance choke valve life in erosive duties. *Wear* **2006**, *261*, 1087–1094. [[CrossRef](#)]
130. Wise, J.L. Geometry and Material Choices Govern Hard-Rock Drilling Performance of PDC Drag Cutters. In Proceedings of the Alaska Rocks 2005 40th U.S. Symposium on Rock Mechanics (USRMS), Anchorage, AK, USA, 25–29 June 2005.
131. Eagle Bergmann’s new-generation Cartex cartridge seals benefits from DiamondFace coating. *Seal. Technol.* **2012**, *2012*, 1. [[CrossRef](#)]
132. Available online: <http://eagleburgmannnow.com/ebnow/index.cfm/stories/diamond-coating-increases-service-life-of-mechanical-seals/> (accessed on 5 December 2012).



© 2018 by the author. Licensee MDPI, Basel, Switzerland. This article is an open access article distributed under the terms and conditions of the Creative Commons Attribution (CC BY) license (<http://creativecommons.org/licenses/by/4.0/>).